INFLUENCE OF ENTROPY GENERATION ON PERISTALTIC TRANSPORT OF PSEUDOPLASTIC FLUID IN A CURVED CONFIGURATION

By

ALEEZA TOUQEER

NATIONAL UNIVERSITY OF MODERN LANGUAGES

ISLAMABAD

May, 2024

Influence of Entropy Generation on Peristaltic Transport of Pseudoplastic Fluid in a Curved Configuration

By

ALEEZA TOUQEER

MS MATHS, National University of Modern Languages, Islamabad, 2024

A THESIS SUBMITTED IN PARTIAL FULFILMENT OF

THE REQUIREMENTS FOR THE DEGREE OF

MASTER OF SCIENCE

In Mathematics

To

FACULTY OF ENGINEERING & COMPUTING

NATIONAL UNIVERSITY OF MODERN LANGUAGES ISLAMABAD

THESIS AND DEFENSE APPROVAL FORM

The undersigned certify that they have read the following thesis, examined the defense, are satisfied with overall exam performance, and recommend the thesis to the Faculty of Engineering and Computing for acceptance.

Thesis Title: Influence of Entropy Generation on Peristaltic Transport of Pseudoplastic Fluid In a Curved Configuration

Submitted By: Aleeza Touqeer **Registration #:** 30 MS/Math/S21

Master of Science in Mathematics
Title of the Degree

Mathematics
Name of Discipline

Dr. Hadia Tariq _____
Name of Research Supervisor Signature of Research Supervisor

Dr. Sadia Riaz _____
Name of HOD (Mathematics) Signature of HOD (Mathematics)

Dr. Noman Malik _____
Name of Dean (FEC) Signature of Dean (FEC)

May, 2024

AUTHOR'S DECLARATION

I Aleeza Touqeer

Daughter of Touqeer Hussain

Registration # 30 MS/Math/S21

Discipline Mathematics

Candidate of **Master of Science in Mathematics** at the National University of Modern Languages do hereby declare that the thesis **Influence of Entropy Generation on Peristaltic Transport of Pseudoplastic Fluid in a Curved Configuration** submitted by me in partial fulfillment of MS Mathematics degree, is my original work, and has not been submitted or published earlier. I also solemnly declare that it shall not, in future, be submitted by me for obtaining any other degree from this or any other university or institution. I also understand that if evidence of plagiarism is found in my thesis/dissertation at any stage, even after the award of a degree, the work may be cancelled and the degree revoked.

Signature of Candidate

Aleeza Touqeer

Name of Candidate

May, 2024

Date

ABSTRACT

Title: Influence of Entropy Generation on Peristaltic Transport of Pseudoplastic Fluid in a Curved Configuration

This thesis is primarily focused on examining the influence of magnetohydrodynamic (MHD) effects on the peristaltic motion of a pseudoplastic fluid within a curved channel, while also considering entropy generation. The formulated problem is addressed through the application of the perturbation technique. The incorporation of commonly accepted assumptions, such as low Reynold numbers and long wavelength, serves to streamline the complexity of the problem. Utilizing MATHEMATICA software, the study presents graphical representations of streamline patterns, velocity distribution, temperature profiles, and entropy variations to provide insights into the interplay of MHD effects within the pseudoplastic fluid under consideration.

TABLE OF CONTENTS

Table of Contents

LIST OF FIGURES

LIST OF SYMBOLS

S	Extra Stress Tensor
ρ	Density
P	Pressure
A	First Rivilin Ericksen Tensor
τ	Shear Stress
μ	Dynamic Viscosity
R	Curvature parameter
r	Radial Direction
x	Axial Direction
c	Wave Speed
λ_1	Wavelength
M	Magnetic Field
ψ	Stream Function
u	Velocity in axial Direction
v	Velocity in Radial Direction
Re	Reynold Number
η	Peristaltic Wall
ϵ	Amplitude
k	Curvature
ϕ	Inclination of Magnetic Field
δ	Wave number
d_1	Channel thickness
D	Mass diffusivity
T	Fluid temperature
K_T	Thermal diffusion ratio
C_ρ	Specific heat
T_0	Temperature at lower wall
T_1	Temperature at upper wall
σ	elastic tension

ACKNOWLEDGMENT

I begin by expressing my profound gratitude to Almighty Allah, whose guidance has made this study both possible and successful. The completion of this study would not have been achievable without the sincere support extended from various sources, for which I am truly thankful. I am particularly indebted to those who played significant roles in my success, with special mention to my research supervisor, Dr. Hadia Tariq. Her unwavering commitment and thorough guidance throughout my research journey were instrumental in the accomplishment of this endeavor.

I shall also acknowledge the extended assistance from the administrations of the Department of Mathematics who supported me all through my research experience and simplified the challenges I faced. For all whom I did not mention but I shall not neglect their significant contribution, thanks for everything.

DEDICATION

I dedicate this thesis to my loving family, whose unwavering encouragement and sacrifices have been the driving force behind my academic journey. Your support has been my anchor, and this achievement is as much yours as it is mine.

To my mentors and educators, your guidance has been invaluable. Your wisdom and encouragement have shaped my intellectual growth, and I am grateful for the knowledge and insights you have shared with me.

CHAPTER 1

INTRODUCTION

1.1 Introduction

The word "fluid" is used in physics and engineering to refer to a condition of matter that may flow and adapt to the geometry of its container. Fluids possess a quality termed fluidity that enables them to move and deform when subjected to external forces, in contrast to solids, which have a fixed shape and volume. This characteristic results from the absence of long-range ordering of the fluid's constituent particles or molecules.

The word "fluid" refers to both gases and liquids. Water, oil, and mercury are examples of liquids that have a known volume and may flow freely. A substance that flows or constantly deforms under outer shear stress is referred to as a fluid in physics. Fluids are materials that cannot withstand any shear force because they have zero shear elasticity.

The definition of the term "fluid" varies by scientific discipline, despite the fact that it typically encompasses both the liquid and gas phases. Also, different fields have different definitions of what it means to be solid, and some things can be both plasma and solid. Fluid, which is broader than the term "hydraulic oil," is a term used in hydraulics to describe liquids with particular properties. Many fields of science and technology, including the fields of physics, chemistry, mechanical engineering, building engineering, and aviation engineering, depend on hydraulics, or the study of flows. Designing effective systems and buildings, forecasting weather patterns, creating transportation systems, and examining fluid motion in biological systems all require an understanding of how fluids behave.

The restoration forces of solids counteract shear, compressive, and tensile stresses. Ideal fluids, on the other hand, only react to ordinary pressures with restoring forces or tension: Compressive stress, which is high pressure, and tensile stress, which is lower pressure, may

both be applied to fluids. Tensile strengths exist for both solids and liquids and when they are surpassed, cavitation in liquids and irreparable deformation in solids occur.

1.2 Non-Newtonian Fluid

The straightforward correlation between shear stress and shear rate seen in Newtonian fluids is defined by non-Newtonian fluids. These fluids' viscosities can alter over time or in reaction to shear forces. They demonstrate a range of flow behaviors, including shear-thinning, where viscosity drops with a growing shear rate, shear-thickening, where viscosity rises with a growing shear rate, and more complex and time-dependent reactions. Non-Newtonian fluid viscosity is often governed by the shear rate or the duration of stress-induced shear deformation. Despite having shear-independent viscosities, certain non-Newtonian fluids exhibit non-standard stress-difference trends or other non-Newtonian characteristics. Non-Newtonian fluids exhibit different connections between shear stress and shear rate than Newtonian fluids, which have a constant coefficient of viscosity. In certain cases, their viscosity can even vary with time. This dynamic behavior makes it impossible to establish a fixed viscosity coefficient. While viscosity is a common descriptor for shear behavior in fluid mechanics, it may not adequately capture the characteristics of non-Newtonian fluids. Using specialized equipment that link stress and strain rate tensors beneath various flow situations, such as oscillating shear or extensional circulation, may be taken into account to provide a more precise understanding. These features can be better understood using tensor-valued constitutive problems, which are often used in continuum mechanics studies. Non-Newtonian fluids can be categorized based on their flow behaviors:

1. **Shear-thinning (Pseudoplastic) Fluids:** As the shear rate rises, these fluids lose some of their viscosity. Paints, ketchup, and shampoos are among examples.

2. **Shear-Thickening (Dilatant) Fluids:** As the shear rate increases, these fluids become more viscous. This behavior may be seen in a few industrial mixes, including slurries and cornflour-water mixtures.

3. **Bingham Plastic Fluids:** These fluids behave as solids until a specific shear stress, known as the yield stress, is exceeded. They demonstrate a linear connection between

shear stress and shear rate after reaching the yield stress. Examples include different drilling fluids and toothpaste.

4. **Viscoelastic Fluids:** These fluids possess both viscosity and elasticity, capable of storing and releasing energy. Their elasticity and viscosity exhibit time-dependent changes. Gels, polymer solutions, and various biological fluids fall under this category.

1.3 Pseudoplastic Fluid

A non-Newtonian fluid known as a pseudoplastic fluid changes in viscosity and fluidity as the shear rate rises. Pseudoplastic fluids have a characteristic known as shear-thinning behavior, in contrast to Newtonian fluids, which retain a constant viscosity independent of shear rate. This specifies that the viscosity of the fluid lowers as it is subjected to increased shear rates or forces, facilitating easier flow.

Mathematical models like the power-law model and the Ostwald-de Waele model are frequently used to describe the behavior of shear-thinning (pseudoplastic) fluids. These models establish a connection between shear stress and shear rate, where shear rate represents the rate of velocity change within the fluid, and shear stress quantifies the applied force. The expression of Power law model is $\tau = K \times \gamma^n$, where γ is the shear rate, τ is the shear stress, *K* is the consistency index, and *n* is the flow behavior index. The degree of pseudo-plasticity is determined by the number of *n*, with values less than 1 indicating a pseudoplastic fluid.

Pseudoplastic fluids are used in a variety of commercial and domestic settings. Ketchup, mayonnaise, and chocolate syrup are just a few examples of the numerous culinary ingredients that display pseudoplastic behavior. Ketchup flows smoothly when pressure is applied to a bottle of it because shear stress causes the viscosity to decrease. The fluid returns to its greater viscosity state after the pressure is released, preventing it from flowing too quickly.

A fluid flow line or conduit with a curved or curved segment is referred to as a "curved channel." The channel is curved or bent rather than straight, and this can have an impact on the properties and behavior of fluid flow inside it. Rivers, pipes, ducts, and pipelines are examples of natural and artificial systems that contain curved channels**.** Centrifugal forces are introduced by a

channel's curvature, which affects the fluid passing through it. Changes in velocity, pressure, and flow patterns occur as a result of the fluid evacuating from the internal curve of the tunnel due to these centrifugal forces. On the outside curve of the channel, the fluid experiences higher speeds and lower pressures, whereas, on the inner curve, it experiences lower velocities and higher pressures. Numerous variables affect how fluid flow behaves in curved channels, including:

1. Curvature: The radius of curvature of the curve has a significant impact on the flow's behavior. Stronger centrifugal forces, sharper bends, and smaller radius of curvature result in more significant flow disruptions and pressure changes.

2. The amount of Reynolds number, which is the fluid's relation of inertial to viscous intensity, has an impact on the flow regime in the curved tunnel. At low Reynolds numbers, the flow is typically laminar, with uniform, well-organized fluid layers. At high Reynolds numbers, the fluid motion can become chaotic and irregular, causing the flow to become turbulent.

3. Rate of flow: The behavior of the flow is influenced by the fluid's flow rate or volume as it moves through the curved channel. More significant flow disturbances, drops in pressure, and shifts in the distribution of velocity can occur at higher flow rates.

4. Channel quality: The channel walls' roughness may have an impact on the flow characteristics. Rough surfaces or abnormalities in the flow might create extra frictional losses.

The existence of a curved channel may have practical ramifications in a variety of situations. For instance:

• Curved channel design is crucial in hydraulic engineering for maximizing flow dispersion, reducing erosion, and effective water transportation.

• Curved channels in transport networks like roads and railroads can impact the flow of air or fluids around vehicles, impacting aerodynamic performance and stability.

• Additional pressure drops, energy losses, and flow instabilities may be caused by the presence of curved portions in fluid transport tubes, which must be considered during system design.

1.4 MHD

MHD, or magnetohydrodynamics, is an interdisciplinary branch of physics that studies the conductivity of electrically conducting fluids such as plasmas, liquid metals, and some ionized gases. To comprehend the interplay between fluid motion and magnetic fields, it combines the principles of magnetism with fluid dynamics.

In MHD, the fluid is viewed as a conducting medium that can be affected by magnetic fields, as well as the other way around. Key equations in MHD combine the Navier-Stokes equations, which control fluid flow, with Maxwell's equations, which describe electromagnetic fields. These equations explain how magnetic fields change over time as well as how fluid mass, momentum, and energy are conserved. Due to their complexity, computational simulations are frequently needed to analyze these equations. The simplest type of MHD, known as ideal MHD, operates under the presumption that the resistive term in Ohm's law is so tiny in relation to the other terms that it may be taken to equal zero. This happens at the limit of high magnetic Reynolds numbers, where magnetic induction triumphs over magnetic diffusion, at the velocity and length scales under concern. perfect processes—processes in perfect MHD that transform magnetic energy into kinetic energy—thus cannot produce heat or increase entropy. Ideal MHD is based on a fundamental concept known as the frozen-in-flux theorem. The bulk fluid and embedded magnetic field are said to be "tied" or "frozen" to one other since they are both confined to flow in tandem. As a result, two sites in the system will always lie on the same magnetic field line and move with the bulk fluid velocity, even if they are separated by fluid flows. The relationship between the liquid and attractive field stabilizes the location of the attractive field in the liquid; for example, if many attractive field lines are integrated together, they will stay that way as long as the liquid has negligible resistance. Due to the difficulties in reconnecting magnetic field lines, energy can be stored by shifting the fluid or the magnetic field's source.

Many different fields use magnetohydrodynamics. It aids in the comprehension of events in astrophysics and space physics such as star formation, stellar winds, and the behavior of plasmas in space, such as solar flares and coronal mass ejections. Understanding and regulating

the behavior of plasma inside fusion reactors is crucial for fusion energy research in order to achieve sustained and controlled nuclear fusion processes.

Since fluid is regarded as a medium that conducts energy in MHD, electromagnetism influences fluid dynamics may be taken into account. These outcomes result from the interplay of magnetism and fluid velocity. Key MHD features include:

Electromagnetic Induction: When an electrically conducting fluid travels in a field of magnetic attraction, the magnetism causes electrical impulses to flow inside the fluid. The electromagnetic inductive law of Faraday describes this occurrence. In turn, the induced currents produce supplementary magnetic fields that have an impact on the movement of the fluid. The Lorentz force is created by the interplay of the magnetic field that exists and the electrical impulses that are produced in the fluid. The fluid is subject to this force, which changes how it moves. The flow of a liquid can be accelerated, decelerated, or changed due to the Lorentz power, which is parallel to both the flow rate of the liquid and the magnetic field that surrounds it.

1.5 Entropy

Despite having its origins in thermodynamics, the concept of entropy has additional uses in information principles, statistics, and a variety of other fields. Entropy essentially describes how much random or uncertainty a system has. Entropy is a scientific concept and observable physical feature that is commonly related to a state of chaos, and unpredictability. Entropy is a phrase and a concept that is used throughout many academic fields, from classical thermodynamics, where it was originally understood, to the ideas of information theory and the microscopic descriptions of natural processes in statistical physics. Its effects are seen across a number of disciplines, including physics, chemistry, biology, cosmology, economics, sociology, meteorology, and information systems, particularly in the context of information sharing. William Rankine, a Scottish engineer and scientist, made a substantial contribution to our comprehension of thermodynamics and related ideas and introduced the terms "thermodynamic function" and "heat potential" in 1850 to describe this concept. Rudolf

Clausius, a pioneering German scientist in the field, defined thermodynamics in 1865 as the relationship between a small intensity of heat and the prevailing temperature. Initially known as "transformation-content" or "Verwandlungsinhalt" in German, Clausius later formulate the term "entropy" from the Greek word for change. He introduced the term "disgregation" in 1862 to describe the microscopic composition and structure of matter. Entropy not only imposes constraints on the feasibility of processes but also respects the first law of thermodynamics, which is the conservation of energy. The second law of thermodynamics, built upon the concept of entropy, states that isolated systems left to evolve naturally cannot reduce their entropy over time, as they tend to approach a condition of thermodynamic stability where entropy is maximized. Entropy is a unit of measure for the disorder or randomness of energy in a system in thermodynamics. The second law of thermodynamics states that entropy tends to increase over time in an isolated system, which means that energy will ultimately disperse and become more equally distributed. This is frequently referred to as the "arrow of time" or the propensity of systems to shift from an orderly to a disorderly state. Entropy is a term used in information theory to describe how much information is there in a random variable or probability distribution. It symbolizes the typical level of surprise or uncertainty connected to an occurrence or series of events. Entropy is a measure of how uncertain or random something is.

1.6 Thesis contribution

In this thesis, an extensive study of previous research (S. Hina, 2016) is presented. The focus is on essential factors, namely heat and mass transfer characteristics of pseudoplastic fluids subjected to both magnetohydrodynamics (MHD) effects and entropy generation in a curved configuration. The approach involves transforming partial differential equations (PDEs) into ordinary differential equations (ODEs) through appropriate methods and employing a perturbation technique to derive solutions. The computational aspect of the study utilized Mathematica, and the obtained results will be visually presented through graphical representations.

1.7 Thesis organization

This thesis is further divided into the following chapters, which are as follows:

Chapter 2 contains a detailed and comprehensive review of the literature in accordance with recent published articles.

Chapter 3 delves into the essential concepts, regulations, and key ideas crucial for comprehending the upcoming work. The final section of this chapter introduces the mathematical model and perturbation method.

Chapter 4 offers an overview of existing work of (S Hina, 2015). The author has studied the pseudoplastic fluid model in a curved geometry with complaint walls. The lubrication approach has been utilized to study the problem. Perturbation technique has been employed to obtain the analytical solution of the problem.

Chapter 5 In this chapter, the research extends the foundational work of S. Hina (2015) by incorporating the effects of magnetohydrodynamics (MHD) and analyzing the impact of entropy generation within a curved channel.

Chapter 6 contains the conclusion drawn in chapter 5. Future recommendation are also included for the future researches.

In the end, the reference list comprises all the sources utilized in this research endeavor.

CHAPTER 2

LITERATURE REVIEW

Peristalsis, a fundamental physiological mechanism, employs rhythmic contractions and relaxations of smooth muscles to facilitate the movement of substances through organized structures within living organisms. Numerous biological activities, including the operation of the reproductive, urinary, and digestive systems, depend on it. On peristalsis, several researchers have researched and are continuing researching.

Saleem *et al.* [1] supervised a detailed investigation into the numerical research of peristaltic circulation involving a non-Newtonian plasma inside an elongated conduit. Their investigation also looked into the subtleties of heat transport in this particular elliptical duct arrangement. They created mathematical equations to precisely reflect the system under study using the Casson fluid model. They also used the long wavelength approximation and the required transformations to turn the mathematical issue into a dimensionless form, allowing for easier analysis.

Gudekote *et al.* [2] looked into how to incorporate changeable liquid and wall properties into a Rabinowitsch fluid's peristaltic process. The study concentrated on a porous, two-dimensional, irregular channel. Convective conditions were used to analyze the characteristics of heat transfer, while Consideration was given to the walls' slipping hazards while analyzing mass transfer. For this experiment, a mathematical model was created under the extended wavelength and small Reynolds number assumptions. The velocity, streamlines, and concentration problems all had exact solutions, while the temperature problem was solved using a perturbation technique.

Hina *et al.* [3] investigation centered on the peristaltic circulation of an indestructible pseudoplastic substance and the properties of the channel barriers. With a focus on modeling

the relevant equations, the study employed lengthy wavelengths as well as small Reynolds number approaches. As a result, the stream function and the axial speed were found. The research looked closely at the many embedding parameter variations within the issue. The velocity curves' non-circular shape around the curved tunnel center line was interesting to remark.

The sinusoidal circulation of Rabinowitsch solutions in an inclined pipe with a responsive barrier and customizable liquid characteristics was studied by Vaidya *et al.* [4]. In particular, the effect of a temperature-dependent heat exchange was considered as the liquid's viscosity varied over the channel's width. Expressions were produced for a variety of relevant variables, including velocity, friction on the skin coefficient, pressure increase, resistive force, streamline, temperature, and efficiency of heat exchange.

In a study by Ali *et al.* [5], the behavior of fluid circulation within a curved tube was investigated, specifically considering a non-Newtonian sinusoidal flow pattern. They employed a constitutive relationship between pressure and shear velocity suitable for a third-grade fluid, which doesn't adhere to Newtonian behavior. The problem involved dealing with two partial nonlinear differential equations. These equations were combined into one second-order ordinary differential equation including a stream function when there was an association of an extended wavelength and a small Reynolds value. The resultant regressive ordinary differential equation was resolved using Mathematica's shooting technique to find the flow function.

In another work, Rashid *et al.* [6] investigated the effects of a produced magnetic field on the peristaltic action of an inelastic Williamson fluid inside a curved conduit. The wave frame of referencing was used to develop the problem formulation. Using extremely tiny Reynolds numbers and large-wavelength estimates, the Homotopy Perturbation Methodology was used to describe the equation for continuity, induction calculation, and equation of motion. The magnetic force function, generated magnetic field, pressure slope and stream function, voltage density, and other terms have precise mathematical definitions. Graphical representations of the consequences of the embedded parts were used for discussion. Rashed *et al.* [7] performed numerical investigations of the peristaltic mobility of dusty nanofluids in a rounded conduit. For the microscopic liquids and sandy portions, two sets of equations based on partial differential equations were provided, and large wavelength and small Reynolds number

assumptions were taken into consideration. Using the appropriate grid adjustments, the physical domain was converted into a rectangular computing model.

In order to organize the passage of an electrolytic solution, Noreen *et al.* [8] employed, fluids that disobey Newton's law pseudoplastic fluid model as the solvent and concentrated on electroosmotic and peristaltic processes. The governing equations in two dimensions were used to study the electrohydrodynamics of the microcapillaries in the body of a person. Low Reynolds number estimations and Debye-Huckel linearization were applied to handle the growing nonlinear differential system. Statistical methods were used to describe the transport features of flow that are non-Newtonian in nature in rectangular small channels. In order to research heat and mass tranport studies. In the context of metachronal pulses and fluctuating liquid characteristics, In their article, Al-zubaidi *et al.* [9] investigated the movement of cilia in a horizontally inclined channel, considering different fluid types such as Newtonian, Pseudoplastic, and Dilatant materials. The study focused on peristalsis flow along ciliated walls, utilizing a non-Newtonian Rabinowitsch model. The analysis took into account the sliding of the canal's walls and convection at its edges. Salman *et al.* [10] delved into the impacts of magnetohydrodynamics and thermal radiation on peristalsis flow within a pseudoplastic fluid through an inclined and tapering asymmetric conduit with holes. The study also considered the presence of convective boundary conditions on the walls.

In another study, Akhtar *et al.* [11] mathematically explored the effects of heat and mass exchange on peristaltic circulation within an elliptical conduit. To comprehend the partial differential equations that emerged in the non-dimensional way, a unique mathematical approach was employed. This method led to an accurate analytical result for the temperature, quantity, and velocities pattern. Electroosmosis in the peristalsis of a fluid that is not Newtonian in tiny channels was taken into account. There were three methods: magnetohydrodynamics (MHD), combined convection, and thermal radiation. For a third-grade fluid with an extended wavelength and a relatively small Reynolds number, Tanveer *et al.* [12] constructed momentum, weight, and temperature calculations. In order to demonstrate how a magnetic field affects the transmission of heat, Hasen *et al.* [13] studied the peristaltic circulation of a Rabinowitsch solution through a material containing holes inside the cilia canal.

Rasid *et al.* [14] examined the effects of an artificial magnetic field on the peristaltic movement of an inelastic Williamson liquid in a twisted conduit in a different investigation. The wave framing of reference was used to formulate the problem. Entropy creation has an effect on a system's efficiency since it decreases the system's output. Entropy creation had to be kept to a minimum for the system to work better. Entropy development usually occurs during irreversible processes but not during reversible ones. The rate of entropy generation was maximized using the second law of thermodynamics. The main objective of Chu *et al.* [15] was to lessen the entropy generated by an inclined tube filled with Rabinowitsch fluid. The gyrotactic motile bacteria in a pseudoplastic Williamson nanofluid that was moving over a stretched cylinder under the influence of an angled field that are magnetic were studied by Naz *et al.* [16].

A new mathematical framework that analyses the motion of peristaltic fluid in an elliptic funnel with mass and warmth transfer was founded by Nadeem et al [17]. In a curved shape route, Ali *et al.* [18] looked into the way that transmission of heat influenced the action of the peristaltic of sticky fluid. The supposition of long wavelength and modest Reynolds number were employed to create theoretical models for heat and circulation transfer. When employing the Rabinowitsch plasma paradigm through a tunnel with an extended wavelength and small Reynolds number estimation, Singh *et al*. [19] were interested in the issue of transferring heat and peristaltic circulation of fluids that were non-newtonian.

By taking into account both heat and mass transmission, Magesh *et al.* [20] goal was to present an updated viewpoint on the peristaltic course of a Johnson-Segalman fluid inside an asymmetric tunnel. To make the governing nonlinear equations easier to understand, they used the assumptions of a long wavelength and a moderate Reynolds number. The peristaltic behavior of a Rabinowitsch solution in a sloping porous channel was studied by Vadiya *et al.* [21], who took into consideration differences in the liquid characteristics and convective situations at the boundary surfaces.

In a study by Rajashekhar *et al.* [22], the primary objective was to assess the impacts of changing viscosity and thermal conductivity on the peristaltic flow of a Casson fluid within an inclined porous tube that was subject to convective heating. It is considered that thermal conductivity is temperature dependent and that viscosity changes along the radial axis. Devaki *et al.* [23] evaluated the Non-Newtonian Casson liquid's peristaltic propagation of waves in an

uneven channel with wall characteristics and heat exchange, taking into consideration estimates with low Reynolds numbers and high wavelengths. Climate, stream operation, and velocity may all be calculated analytically using a variety of physical variables. In the research conducted by Sadaf *et al.* [24], the focus was on investigating the peristaltic flow of a Williamson nanofluid within an annular geometry, considering the influence of an externally applied magnetic field. To solve the particular problem at hand, the study employed an approximation of a lengthy wavelength and a relatively small Reynolds number. Abbasi *et al.* [25], on the other hand, delved into the impact of an induced magnetic field on the peristaltic flow of a Carreau-Yasuda fluid within a curved conduit. Also taken into account are hall phenomena.

The thermal evaluation of the dual-stage peristaltic nanofluid movement in the dual-dimensional wavy tube was carried out by Hatami *et al.* [26]. By using the sinusoidal operation, the top, and bottom channel barriers were seen as having a wavy form. A basic understanding of the impact of heat exchange on the flow parameter of a dual-grade dusty flow in an elastic tube with peristaltic circulation was provided by Hafez *et al.* [27]. The connected differential expression was used to simulate the motions of both dust fragments and streams. The primary goal of Saba *et al.* [28] was to simulate and investigate the effects of curvature-dependent duct boundaries on unidirectional sticky material movement via curved dimensions during peristalsis. This is the initial time that numerical modeling for such a flow arrangement has been given. For the mathematical modeling of the issue, assumptions from the lubrication theory are applied.

Mallick *et al*. [29] examined the electro-kinetic peristaltic movement of an Eyring-Powell tiny fluid. It is believed that the flow occurs in an asymmetrical pattern, irregular microchannel. The system is intended to be subjected to Joule heating and to be affected by a magnetic field that is formed outside. Due to their extraordinary ability to transmit heat and prospective uses in engineering and the medical sciences, nanofluids have drawn more interest since Choi's seminal discovery. Since most fluids have non-Newtonian characteristics, Rafiq *et al*. [30] explored this.

In a work by Naz *et al.* [31], a smooth cylinder was intentionally surrounded with Carreau nanofluid. Gyrotactic microorganisms floating in a medium and exposed to an angled magnetic field were present when this was being done. The authors used Von Neumann resemblance transformations to translate paired partial differential equations from their physical

representation into more complex coupled ordinary differential equations. Tanveer *et al.* [32] investigated heat exchange phenomena within a curved conduit characterized by regularly contracting and extending waves along its edges. This study focused on the peristaltic circulation of Carreau fluid. Examining the movement of a second-stage dusty fluid through an elastic tube with sinusoidal moving walls, Tariq and Khan [33] explored the characteristics of this system. By taking into account streamlined conversions, paired equations for the liquid and solid fragments have been modeled. The peristaltic circulation of Jeffery material down an irregular conduit with varying viscous and thermal efficiency is highlighted by Manjunatha *et al.* [34] as being affected by mass as well as heat transfer.

Yasmeen *et al.* [35] addressed the sinusoidal Johnson-Segalman liquid flow in a symmetrically bent channel with convective circumstances and flexible walls. The channel barrier is thought to be compliant. They discussed the impact of mass and heat convection on boundary conditions and the channel's curvature. The constitutive equations for Johnson-Segalman fluid are modeled and investigated using the lubrication approach.

Gnaneswara *et al.* [36] studied the influence of spinning and heat transfer on the magnetohydrodynamic (MHD) peristaltic motion of a Jeffrey liquid in an asymmetric tunnel featuring partial slip. In a two-dimensional tunnel, Javed *et al.* [37] explored the effects of heat transfer on the MHD sinusoidal movement of a contaminated fluid according to Saffman's model.

Shukla *et al.* [38] conducted an analytical investigation on heat exchange during the peristaltic motion of a Newtonian fluid through an unevenly inclined tunnel, while considering the influence of inner boundary surface roughness. The study placed particular emphasis on analyzing the physical dynamics of various flow characteristics across different magnitudes of surface roughness parameters.

Hayyat *et al.* [39] discussed the peristaltic flow of a Jeffrey fluid through a curved tube, considering convective conditions at the boundary walls for thermal transfer. The study took into account Joule heating and the effects of an applied magnetic field.

Bhatt *et al.* [40] tackled the issue of heat transfer in the peristaltic motion of a viscous incompressible fluid within a two-dimensional irregular channel with a porous boundary under conditions of long wavelengths and low Reynolds numbers. Eldabe *et al.* [41] assessed the influence of non-constant stiffness and magnetohydrodynamics on the sinusoidal motion of nanofluid through a porous medium. Considerations include thermal production, the reaction of chemicals, and ohmic absorption.

Tahir *et al.* [42] investigate the impact of expanding and pseudoplastic characteristics of sinusoidal flow on tiny fluids. Thermal transfer analysis and this behavior are both looked at in an asymmetric, non-uniform tunnel. n this investigation, the Reiner-Philippoff (RPh) fluid theory is employed to describe the non-Newtonian behavior of the fluid. The Reiner-Philippoff fluid theory establishes a connection between stress and the rate of deformation. A clinical instance illustrating the impact of an endoscope on peristaltic flow pertains to the passage of stomach acid when an endoscope is introduced through the small intestine. This example underscores the significance of peristaltic flow in clinical diagnosis. Devakar *et al.* [43] have investigated the impact of magnetohydrodynamics (MHD) on the sinusoidal propulsion of non-Newtonian fluid (considered as pair stress fluid) in a tube made up of an endoscope. Entropy generation is a crucial component of any heat transport advancement and lowers the system's immutability factor.

Numerous traditional industrial areas requiring fluid flows and heat transfer have enormous applications for entropy generation evaluation. In order to evaluate the impact of entropy generation and velocity slip on MHD sinusoidal flow for an incompressible liquid in a diverging tube, Abbas *et al.* [44] adopted a lubrication approach. Multiple applications, including micro thermal exchanger systems, mechanical-electromechanical networks, cooling of electronic equipment, and micro air vehicles, can establish the heat flow in microchannels. Entropy generation minimization is a consideration in heat flow optimization for engineering purposes. The goal of this work is to use EGM to measure the heat exchange of a non-Newtonian magneto-Carreau liquid in a microchannel. In mathematical modeling, the Carreau fluid model is employed. Shehzad *et al.* [45] also looked into convective and Joule heating characteristics.

Rooman *et al.* [46] conducted a study on entropy generation within an upright Riga system, focusing on a reactive Williamson small fluid flow. The formulated model's thermal equation

incorporates considerations for various factors including magnetohydrodynamics (MHD), thermophoresis, nonlinear heat radiation effects, and variations in heat conductivity.

The formation of entropy, the associated with the field that is magnetic, and the combined convection fixed point circulation of a pseudoplastic nanoscale liquid across an elastic medium were all examined by Hou *et al.* [47]. Williamson fluid in the curved tunnel have been investigated by Rashid *et al.* [48]. The problem is built using a wave mode of reference. Under the influence of mass and thermal transfer, the flow theory for two inseparable and incompressible Rabinowitsch plasma with various viscosities was examined by Hasen *et al.* [49]. Sinusoidal has been utilized to build and analyze the pertinent flux motion responsible for the fluid's circulation, and the lubrication technique expression for thermal and mass transfer. The temperature description, the concentration description, the streamline, the velocity description for the inner and outer layers, and the analytical equations for the interface geometry are all obtained.

Hasona *et al.* [50] investigated the impact of temperature-dependent thermal transmission and thermal energy on the peristaltic movement of pseudoplastic microscale fluids within an inclined, asymmetric, and irregular tunnel. This study focused on the three primary modes of heat emission and transfer, namely radiation, conduction, and convection. Consideration is given to the sloped magnetic field. Electrical conductivity behaves in the same way as thermal conductivity under the Wiedemann-Franz equation in metals, and electrons that are freely animated likewise transmit heat energy.

Abd-Alla [51] aimed to investigate whether small gold fragments exhibit free-floating behavior under the assumptions of a large wavelength and a small Reynolds number. The study examined the interplay of thermal and mass transfer, buoyancy effects, thermophoresis, and Brownian motion within a micropolar microfluid flowing through a porous medium in an asymmetric tunnel, all under the influence of a regular magnetic field.

In a tapered and asymmetric tunnel, Hayat *et al.* [52] studied the impact of the Soret and Dufour effects on the sinusoidal flow of a magnetohydrodynamic pseudoplastic microfluid. The investigation also incorporated considerations for thermophoresis, Brownian motion, and first-order chemical reactions.

El-Dabe *et al.* [53] delved into the peristaltic motion of a steady non-Newtonian microfluid with heat transfer through a non-uniform inclined channel. This scenario involved flow through a non-Darcy permeable medium following a power-law behavior. The study also accounted for effects such as thermal radiation, heat generation, Ohmic dispersion, and the presence of a constant external magnetic field. Tiny fluid peristalsis is important for industrial machinery, cancer therapy, and ulcer therapy.

Hayat *et al.* [54] used combined convection and Hall voltage to replicate the MHD sinusoidal transport of Sutterby tiny fluid. For flexible tunnel walls, partial slide and convective circumstances are induced. By taking into account the effects of Joule heating, thermal ray sticky dissipation, and activation energy, energy, and concentration expression were modeled.

Entropy creation and thermo-hydraulic efficiency of a curly channel with three curvature profiles are simulated numerically. For walls with wavy surfaces, sinusoidal, trapezoidal, and triangular forms are regarded as curvature profiles. On entropy formation and the thermo-hydraulic efficiency of a curved channel, the effects of various profiles and Reynolds numbers were addressed by Akbarzadeh *et al*. [55].

Khan *et al.* [56] looked that how entropy is generated in the reactive dissipative circulation of Carreau-Yasuda plasma over an extensible surface using flow parameters such as the Brinkman quantity magnetic variable, diffusion variable, Weissenberg quantity, and the comparison of temperature and concentration variable. The Carreau-Yasuda plasma total entropy formulation was obtained using the 2^{nd} law of thermodynamics. Slide flow in electrical conduction was given into consideration. In the formulation of the energy equation, factors such as Joule heating, heat absorption, and dispersion are also incorporated.

Iqbal *et al.* [57] investigated the influence of entropy generation in the context of the magnetohydrodynamic (MHD) sinusoidal motion of temperature-dependent thermal conduction within a Carreau-Yasuda microfluid. The study showcased the thermophysical attributes of Graphene Nano powder and Ethylene Glycol within a non-Newtonian framework. Using lubrication estimation, the expected flow state is modeled while taking into account sticky decadence, heat origination, Joule heating, thermophoresis impact, Brownian circulation, and slip circumstance.

Hayat *et al.* [58] focused on the sinusoidal transference of a Sutterby plasma with thermal conduction that are dependent on temperature in curvy shapes. A skewed magnetic field is taken into account. Sticky dependence, non-linear thermal rays, variable heat conductivity, Joule heating, and thermal sink effects are included in the modeling of energy expression. A technique for a formulation that considers lubrication has been used. Entropy discusses irregularities in the heat transport process. The effect of combined convection, Hall electric current, and magnetic field on Powell-Eyring tiny fluid peristaltic circulation in the symmetric tunnel was highlighted by Ahmed *et al.* [59].

The effects of heat radiation, ohmic heating, and sticky dependence are all included in the energy expression. To investigate the properties of mini fluids, Brownian movement, and thermophoresis are taken into account. On the boundary barriers, circumstances for velocity slip, heat leap, and zero mass flow are taken into account. A curved structure is used to mimic the peristaltic movement of a Sisko substance with varying properties of heat conductivity and viscosity. Both are regarded as temperature- and space-dependent. Under the assumptions of a small wavelength and high Reynolds numbers, the conservation equations for mass, momentum, and temperature are initially formulated and subsequently simplified. In their investigation of heat exchange anomalies, Bibi *et al.* [60] also incorporated considerations for entropy. The study focuses on the influence of the Hall voltage on the mixed convective sinusoidal flow of a nano liquid within a compliant boundary channel. The porous space is filled by a Brownian movement and thermophoresis composed of nano liquid. Impacts of partial slippage and convective circumstances were examined by Alsaedi *et al*. [61] simultaneously.

The fluid flow produced by the sinusoidal pumping mechanism has many different uses. Javid *et al.* [62] combined the traditional peristaltic flow issue with the intricate curly curved tunnel under magnetic influences as a result of this fact. The first model for the flow issue makes use of the curvilinear coordinate scheme. In order to convert the issue from the static frame to the dynamic frame, Galilean transformations were employed. Since the complex phase in a narrow-gapped tunnel causes creeping flow, we may use a small Reynolds number and the lubrication estimation.

Tariq *et al.* [63] examined the impact of various peristaltic factors on the flow of second-grade dusty fluid via a curved design. Modeling the distinct set of solutions for the liquid and dust

fragments using stream parameter conversions. The peristaltic circulation of tiny fluids in a vertical uneven channel is investigated by Ellahi *et al.* [64] through analysis. A novel model is suggested for the nanoscale concentration, whereas the mathematical approach under consideration uses continuity and momentum calculations. We concentrate primarily on Ag- and Cu-water tiny liquids. Together with the porous nature of the medium, the impacts of entropy production are also taken into consideration. An important outcome of considering a thermal conductivity theory concerning Brownian motion in nanofluids is the dependence of particle size, volumetric proportion, and temperature response on the theory itself. The primary aim of Saba *et al.* [65] was to evaluate the impact of the curved geometry of channel edges on the magnetohydrodynamic (MHD) peristaltic flow of a viscous fluid, with specific implications for heat transfer. The results of the investigation are provided by considering the impact of Joule, Hall currents, and sticky dissipations. In addition, the temperature and no-slip momentum are considered. The implications of longer wavelength and lower magnetic Reynolds count schemes are applied to the computational framework. The problem is transformed from an experimental frame to a wave context via the Galilean conversion. Every heat transport process must include the production of entropy. It helps to reduce the irreversibility rate of a system. Entropy generation through analysis is essential in many conventional industrial fields where heat transport and fluid fluxes are involved. The current study's main objective is to analyze how entropy is produced when nanofluid is circulated through an unequal channel using the peristaltic process. The governing equations took into consideration the effects of thermophoresis, hybrid convection, and Brownian motion. Akbar *et al.* [66] also brought up the viscosity's sensitivity to temperature. Analyzing nanofluids is done using the Buongiorno model. The mathematical modelling includes an extended wavelength estimate.

CHAPTER 3

BASIC DEFINITIONS AND FORMULAS

This chapter contain basic definitions taken from book “FLUID MECHANICS” by Frank M. white [67].

3.1 Newton’s law of Viscosity

A fundamental idea in fluid dynamics, Newton's law of viscosity, or Newtonian viscosity, describes the connection between a fluid's shear stress and shear rate. The shear stress (τ) that a fluid experience is directly commensurate to the fluid's velocity gradient $\frac{du}{dy}$,where denotes the shear stress and $\frac{du}{dy}$ denotes the velocity slope perpendicular to the administration of flow. It has the following mathematical expression:

$$\tau = \frac{du}{dy}.$$

The fluid's dynamic viscosity in this equation stands for the fluid's internal resistance to shearing. It gauges the fluid's thickness or flow resistance. The fluid is more resistant to shear deformation the higher the dynamic viscosity. The speed at which adjacent fluid layers slide past one another is represented by the shear rate $\frac{du}{dy}$. It is the velocity gradient that is parallel to the flow direction. Fluids that display a direct connection between shear rate and shear stress are cited as fluids that are Newtonian and are subject to Newton's law of viscosity. Regardless of the shear rate or applied shear stress, the dynamic viscosity in Newtonian fluids is constant. Newton's law of viscosity can be used to analyze and forecast the flow behavior of these fluids since shear stress and shear rate have a linear relationship. For Newtonian materials, which are liquid with a linear connection between the stress generated by shear and the velocity shift,

Newton's equation of stickiness is valid. In other words, irrespective of the rate at which shear occurs or the applied shear stress, Newtonian substances have a viscosity that remains stable. Water, air, and the majority of the gaseous and liquid substances that are encountered in daily life are typical examples of fluids that are Newtonian. It's significant to remember that not all materials adhere to Newton's viscosity principle. The viscous behavior of fluids that aren't Newtonian, including some kinds of pastes and polymers, is more complicated.

Numerous applications in science and engineering depend on Newton's principle of viscosity. It aids in the design of types of machinery like pumps and other components and compressors as well as the knowledge of fluid flow behavior in pipes, routes, and other structures. The creation of more intricate rheological models that represent fluids that are not Newtonian, which displays various viscosity characteristics under various shear situations, is also supported by this research.

3.2 Time-Independent Fluid

A time-independent fluid, commonly referred to as a steady-state fluid, is a fluid flow in which the fluid's characteristics and behavior do not alter over time. In other words, there are no temporal fluctuations in the fluid flow, which is constant. Any point in a fluid with temporal independence will always have the same velocity, pressure, and other attributes. This indicates that the characteristics of the fluid flow remain constant as it passes through a system or a region. The steady flow of water through a conduit with a fixed diameter and length is a typical example of a time-independent fluid flow. The fluid will maintain a steady flow profile with the same velocity and pressure at any given location along the pipe if the flow rate stays constant and there are no external impacts, such as changes in pressure or temperature. Equations that control the behavior of the fluid, like the continuity equation can be used to describe this steady state. The velocity, strain, density, and various other parameters of the medium at any given instant in time are stable in a time-independent movement of the fluid. This consistency holds true for both these attributes' magnitude and direction. The properties of the fluid flow remain unchanged as it passes through an object or area. Let's look at an illustration of stable-state water movement via a pipe to more fully comprehend time-independent hydraulic fluxes. At any given location along the pipe, fluid parameters like pressure and speed will also remain fixed if the flow rate stays constant. Consider a situation where water is continuously flowing through

a horizontal pipe at a constant flow rate and constant pressure gradient. The fluid's behavior continues to be time-independent in the absence of changes to variables like the pipe's diameter, the viscosity of the fluid, or the pressure levels. Low Reynolds numbers, a measure of the proportion of viscous forces to inertial forces in the fluid, are a distinctive feature of this type of flow. As a result, a steady and uniform laminar flow pattern develops. It's crucial to understand that, even though this hypothetical situation is an idealized one, real-world circumstances can cause time-independent behavior to diverge. It is implied by this steady-state condition that the flow parameters do not alter over time. Stable-state equations are frequently used in mathematics to explain time-independent movements of fluids. The continuity computation, which connects fluid velocity with the cross-sectional dimension, is constant for fluids with no compression. Another essential equation for describing steady-state fluid flows is the Bernoulli calculation, which links the fluid's flow rate, pressure, and inclination. Many engineering and scientific endeavors take advantage of the time-independent movement of fluids premise. It makes computations and analysis simpler, enabling engineers to create less complicated systems and materials. It also helps in forecasting how fluids would behave under steady-state circumstances.

3.2.1 Types of Time-Independent Fluid

Time-independent fluid comprises two types:

i. Steady-state Flow

Steady-state flow refers to the behavior of a fluid in which its characteristics are constant at any given moment. This implies that characteristics such as velocity, pressure, and other characteristics are constant throughout the fluid. Usually, stable systems with predictable flow rates and circumstances exhibit this type of flow. As long as these circumstances are not changed, for instance, water flowing through a conduit under constant pressure as well as flow rate exhibits steady-state flow.

ii. Laminar Flow

Laminar flow is a particular kind of steady-state flow that features orderly and uniform fluid particle motion. These particles move in parallel layers, or "laminae," with little mixing between neighboring levels in the flow of laminar particles. Low Reynolds numbers, which represent a

fluid's ability to balance inertial and viscous forces, are indicative of this behavior because it happens at comparatively low velocities.

3.3 Time-dependent Fluid

A fluid flow in which the fluid's characteristics and behavior change over time is referred to as a time-dependent fluid, also known as an unsteady or transient fluid. Contrary to a time-independent fluid, a time-dependent fluid's properties vary continually as it passes through a system or area. The velocity, pressure, and other variables at a particular place in the fluid flow change over time in a time-dependent fluid flow. This may happen as a result of a number of things, including modifications to the boundary conditions, fluid characteristics, external forces, or the introduction of disturbances into the system. Fluid flows that depend on time can behave in complex and dynamic ways. For instance, a fluid will begin to flow and accelerate when a rapid pressure differential is provided while it is originally at rest. The velocity, pressure distribution, and other characteristics of the fluid will alter over time until a new equilibrium or steady state is attained. knowledge of transitory processes, dynamical flows, and structures that adapt or change over time requires knowledge of time-varying liquids. varies in boundary conditions, outside influences, fluid characteristics, or beginning circumstances are just a few examples of the many variables that may affect how fluid behavior varies over time. The Navier-Stokes equation and other mathematical models of fluid behavior must be taken into account in their whole form, which includes time-varying terms when analyzing time-varying fluids. These formulas offer an analytical framework to represent and examine the time-dependent behavior while also describing the conservation of energy, motion, and mass in the liquid. A variety of phenomena, such as vortex loss, transmission of waves, instability, and temporal processes, can be seen in time-varying fluid flows. The rogue flow over an airfoil, the behavior of waves in the sea, the movement of a chaotic jet, or the filling and draining of a tank are illustrations of time-dependent fluid movements. Numerical techniques, such as computing fluid dynamics (CFD), are frequently used to study time-varying fluids. These techniques take into consideration the fluid's time-varying characteristics by discretizing the formulas that govern and solving them repeatedly at various time increments. CFD simulations may aid in the design and management of several engineering systems as well as offer in-depth insights into the motion of time-dependent fluids. It's essential to comprehend time-dependent materials in many real-world situations. For instance, in aerodynamics, research of unstable fluid

behavior is crucial for designing airplanes because it enables the investigation of how an aircraft interacts with the wind during maneuvers or roughness. The time-dependent movement of fluids is essential for understanding variations in the weather, ocean currents, and pollutant distribution in the field of environmental science. The movement of time-dependent liquids in manufacturing operations is crucial for maximizing the efficiency of thermal exchangers, ignition systems, and reactors for chemicals. The turbulent airflow around a moving vehicle serves as an example of a time-dependent fluid. The fluid's properties, including velocity, pressure, and density, change dynamically as the vehicle moves through the air in both the temporal and spatial dimensions. Fluid motion that is chaotic and unpredictable and is characterized by variations in these characteristics is referred to as turbulent flow. Imagine a car driving down a road at a high rate of speed. Due to the construction of the vehicle, its speed, and outside forces like wind gusts, the air surrounding the vehicle sees rapid fluctuations in both velocity and pressure. In this case, the motion and interactions of fluid particles adopt complex patterns, leading to unpredictable flow behavior. The constant changes in fluid properties caused by the movement of the vehicle give this turbulent flow its time-dependent characteristics. In comparison to the steady and smooth laminar flow, modelling and analysis of turbulent flow are much more complex.

3.4 Law of conservation of Mass

The rule of conservation of mass, which governs physics, stipulates that the overall mass of a closed system stays constant across time. It suggests that mass can only be rearranged or modified, not generated or destroyed. This rule states that the total mass of all the objects or substances involved at the start of any physical or chemical process will equal the total mass at the completion of the process. This idea applies to a broad variety of events, from straightforward mechanical interactions to intricate chemical processes. The concept of the conservation of energy is strongly related to the law of conservation of mass. Einstein's theory of relativity shows that mass and energy are connected, and that mass may be changed into energy and vice versa. The total mass energy in a closed system, however, does not change even when mass is transformed into energy. The law of conservation of mass presumes an isolated system with no mass interaction with the environment, which is a crucial point to remember. Since there are frequent interactions with the environment, achieving a totally

isolated system might be difficult in practice. The law of conservation of mass is still a crucial idea for comprehending and anticipating how matter will behave in a variety of physical processes. It is important to note that the idea of mass conservation has been broadened in contemporary physics to encompass the preservation of other physical properties, such as electric charge, momentum, and angular momentum. These rules, which are commonly referred to as conservation laws, are the cornerstone of several scientific fields and are essential to comprehending the basic laws of nature. General continuity equation:

$$\frac{\partial \rho}{\partial t} + \nabla \cdot (\rho \vec{v}) = 0$$

3.5 Law of Conservation Energy

A fundamental idea in physics is the concept of conservation of energy, commonly referred to as the principle of energy conservation. It asserts that the total energy level in a system that is closed remains constant throughout time. Energy cannot be created or destroyed; it can only be transformed from one form to a different one or transported across systems.
Scientists have contributed to the idea of energy conservation throughout history, but until the 19th century that it became formalized and widely recognized. Hermann von Helmholtz, a German scientist who created the first law of thermodynamics, usually referred to as the law of energy conservation, was one of the principal developers of this idea. Energy is always preserved in all physical processes, according to the rule of conservation of energy. It includes a variety of energy types, such as nuclear, chemical, electromagnetic, thermal, mechanical, and thermal energy. Although these many types of energy can be transformed into one another, the overall amount of energy in a closed system never change proving that energy is conserved. This idea is valid for many physical processes, including heat transport, chemical reactions, nuclear reactions, and mechanical interactions. The overall energy of the system, for instance, remains constant in a swinging pendulum while potential energy is transformed into kinetic energy and vice versa (presuming no energy losses due to friction or other reasons). While the concept of conservation of energy is a key idea, it should be noted that this does not mean that energy is always fully used or transformed effectively. Real-world situations may involve energy losses as a result of friction, air resistance, or ineffective energy conversion techniques. However, the overall energy of an isolated system, when no additional or diminished external

energy is present, remains constant. A fundamental principle of physics, the rule of conservation of energy is essential to comprehending and forecasting the behavior of natural processes. It serves as the foundation for the creation of many scientific ideas and concepts, such as electromagnetism, quantum mechanics, and thermodynamics.

General Energy equation:

$$\rho\, c_p \left(\frac{dT}{d\bar{t}} + (\vec{v}.\nabla)T\right) = k\,\nabla^2 T + Q$$

3.6 Laws used in MHD

The science of magnetohydrodynamics (MHD) examines the behavior of liquids that are conducting electricity in the presence of magnetic fields. It mixes electromagnetic and fluid dynamics ideas to explain the trade between the fluid and the glamorous field. MHD analyses and models these relationships using a number of laws and equations. The fundamental rules and equations then employed in MHD

3.6.1 Conservation regulations

According to the theory of conservation of mass, the weight of a fluid in an enclosed structure stays constant. According to the continuity equation, the divergence of the mass flux density v and the rate of change in mass density with respect to time *t* must both equal zero.

$$\frac{\partial \rho}{\partial t} + \nabla \cdot (\rho \vec{v}) = 0$$

The fluid's velocity is indicated here by the letter $\vec{v}$.

3.6.2 Energy conservation

According to this principle, a fluid's overall energy is conserved. In MHD, it is typical to think of the total energy as the product of the kinetic energy and the internal energy (caused by temperature). The energy equation, which contains equations for heat conduction, work done by pressure, and energy dissipation owing to viscosity and resistance, explains the conservation of energy.

3.6.3 Maxwell Equation

The behavior of electromagnetic fields and their interactions with charged particles is described by Maxwell's equations. There are four Maxwell equations.

1. Gauss law for electricity

$$\nabla . \boldsymbol{E} = \frac{\rho}{\epsilon_0}$$

This law states that the electric flux through a closed surface is proportional to the charge enclosed within that surface. Here, $\boldsymbol{E}$ is the electric field, ρ is the charge density, and $\epsilon_0$is the permittivity of free space.

2. Gauss law for Magnetism

$$\nabla . \boldsymbol{B} = 0$$

This law indicates that there are no magnetic monopoles; the net magnetic flux through a closed surface is zero. In other words, magnetic field lines are always continuous loops, and $\boldsymbol{B}$ is the magnetic field.

3. Ampere law

$$\nabla \times \boldsymbol{B} = \mu_0 \boldsymbol{J} + \mu_0 \epsilon_0 \frac{\partial \boldsymbol{E}}{\partial t}$$

This law shows that magnetic fields are generated by electric currents $\boldsymbol{J}$ and by changing electric fields. Here, μ_0 is the permeability of free space.

4. Faraday law

$$\nabla \times \boldsymbol{E} = -\frac{\partial \boldsymbol{B}}{\partial t}$$

Faraday's Law states that a changing magnetic field over time creates an electric field. This is the principle behind electromagnetic induction, which is the working principle of many electrical generators and transformers.

The Lorentz force law and a set of partial differential equations known as Maxwell's equations, sometimes known as Maxwell-Heaviside equations, serve as the conceptual pillars of traditional optical technology, electrical wiring, and electromagnetism. The equations provide a mathematical description for wiring, optical signals, and broadcast technologies such as power generation, motors powered by electricity, communication via wireless networks, optics, radar, etc. They explain how charges, currents, and changes in the fields produce electric and magnetic fields. James Clerk Maxwell, a mathematical expert, and physicist, presented a draught of the formulas in 1861 and 1862 that included the Lorentz force theory.

3.6.3 Gauss law for magnetism:

The magnetic field produced by a band of current illustrates the principle of Gauss for magnetic forces, which asserts that magnetic field paths never start or end and instead cycle or carry on forever. According to Gauss's theory of magnetism, magnetic monopoles, which are analogous to electric charges, do not exist independently as north or south magnetic poles. Instead, a dipole is thought to be responsible for a material's magnetic field, and a closed surface has no effect on the magnetic field's net outflow. Magnetic dipoles can be represented as circles of current or as indestructible pairs with comparable and opposing "magnetic particles". The total magnetic flux over a Gaussian surface is approximately 0 since the field of magnets is a solenoidal vector source.

3.6.4 Ohm's law

Ohm's law connects the fluid's resistivity and the electric field's *E* and *J* current densities. The foundation for understanding and simulating the behavior of electrically conducting fluids in the presence of magnetic fields is laid forth by these rules and equations. Different MHD processes, including magnetic reconnection, magnetohydrodynamic waves, and plasma confinement, may be analyzed and understood by solving these equations with the proper boundary conditions.

3.7 Laws used in entropy

In the study of thermodynamics, the entropy law is the name given to the second principle of thermodynamics. The second principle states that the entropy of an isolated system never decreases and always tends to increase with time or remain constant in reversible processes.

Entropy measures the energy distribution and the variety of microscopic states that a system may take at a certain macroscopic state. The entropy of a highly organized and ordered system is low, while that of a chaotic and random system is large.

There are two primary effects of the second law of thermodynamics:

Increase in Entropy: In an isolated system, the overall entropy has a propensity to rise with time. This indicates that energy tends to diffuse across natural processes, and systems end up being more disorganized or erratic. The "arrow of time" is a term used to describe this discovery, which relates to the idea of irreversibility in natural processes.

Reversible processes, in which the system goes through changes that may be undone by extremely minute adjustments, are characterized by entropy conservation. Although idealized and seldom in reality, reversible processes provide a valuable framework for examining and comprehending thermodynamic phenomena. Probabilities and the number of potential microscopic states can be used to explain the growth in entropy. Entropy tends to rise as a system develops because it seeks to experiment with tiny configurations or arrangements. On the other hand, entropy increases in the environment are frequently the consequence of efforts to decrease or improve order, which involve energy and work.

It is important to note that localized entropy drops are not prohibited by the second rule of thermodynamics. Entropy can momentarily decrease in a particular region, such as a living thing or a process that is affected by outside energy. But the overall entropy of the system and its surroundings either rises or stays the same. Beyond thermodynamics itself, the idea of entropy and the second rule of thermodynamics have significant ramifications. They offer a framework for comprehending the direction and behavior of natural processes, making them pertinent to disciplines like information theory, cosmology, and the study of complex systems.

3.8 2nd Law of Thermodynamics

A cornerstone of physics, the second rule of thermodynamics regulates the flow of heat and the effectiveness of energy conversion in thermodynamic processes. Although it may be expressed in a variety of ways, the Clausius formulation is one of the most popular:

It is impossible for a process to produce only the transfer of heat from a colder to a hotter body. By stating that heat naturally travels from a site of greater temperature to an area of lower temperature, this proposition emphasizes the irreversibility of some processes. The second law defines entropy as a metric for the disorder or unpredictable nature of a system. The second law of thermodynamics is related to a few essential ideas:

Entropy is a measurement of a system's unpredictability or disorder and is represented by the letter *S*. The overall entropy in a closed system usually rises over time or stays constant in reversible processes. It signifies that systems have a propensity to develop toward a state of greater chaos or equilibrium.

Entropy Change: According to the second rule of thermodynamics, an isolated system's entropy can never decrease, whereas it grows during an irreversible process. Entropy change (*S*) for a reversible process is determined by the equation $S = \frac{Q}{T}$, where Q stands for heat transfer and T for absolute temperature.

3.8 Lorentz Force

When a charged particle travels through an electromagnetic field, the Lorentz force, also known as the electromagnetic force, emerges. Hendrik Lorentz, a Dutch scientist who made a substantial contribution to the development of electromagnetic theory, is honored by having his name given to this idea. The electric force and the magnetic force are two essential components of the Lorentz force. A charged particle is propelled in the direction of the field by the electric force, which develops as a result of the existence of an electric field. The force operates in the same direction if the particle's charge is in line with the field's polarity; otherwise, it acts in the opposite direction if the charge is in opposition to the field's polarity. On the other hand, when a moving charged particle enters a magnetic field, the magnetic force is activated. This force acts at a right angle to the magnetic field's direction and the speed of the particle. The Lorentz force is a fundamental concept in electromagnetism, embodying the complex interaction between electric and magnetic forces on charged particles in electromagnetic fields.

CHAPTER 4

ON PERISTALTIC MOTION OF PSEUDOPLASTIC FLUID IN A CURVED CHANNEL WITH HEAT TRANSFER AND WALL PROPERTIES

4.1 Introduction

In this chapter, we have reviewed the paper of Hina *et al.* [68], "On peristaltic motion of pseudoplastic fluid in a curved channel with heat/mass transfer and wall properties". In this article, they discussed the combined effects of wall characteristics and heat/mass exchange. By assuming that the peristaltic wave has a longer wavelength than the channel's mean half-width, the mathematical representation is made simpler. It is possible to construct series solutions for stream function, temperature, and species content. The profiles of the curvy duct are not symmetrical about the center line like they are in the scenario of a plane channel. The upper and lower parts of the curved channel's higher and lower portions of the stuck bolus are different sizes. Additionally, as the case of a plane channel is approached, the amount of circulations increases/decreases in the upper/lower portion of the channel.

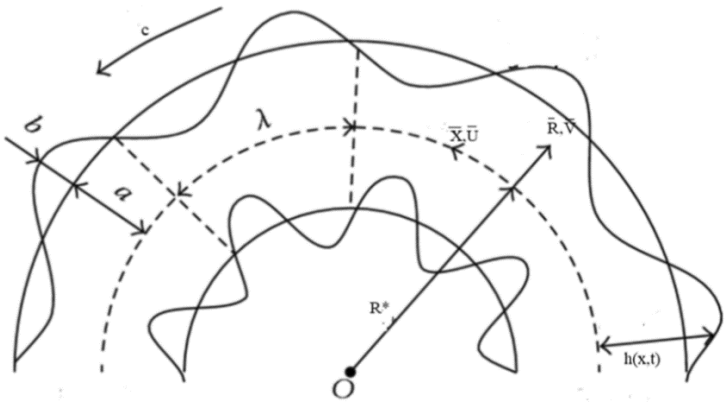

Fig. 4.1: The geometry of the channel.

4.2 Mathematical Formulation

We take into account the peristaltic movement of a pseudoplastic liquid in a curved channel with a thickness of $\tilde{d}_1$. The flow has a longitudinal direction of $\tilde{x}$ and a radial path of $\tilde{r}$. $\tilde{u}$ and $\tilde{v}$, respectively, are the elements of velocity in the longitudinal and peripheral directions. The waves that are being propagated have a sinusoidal form, which may be described by equations

$$\tilde{\mathrm{r}} = \pm\eta(\tilde{x},\tilde{t}) = \pm\left[\tilde{d}_1 + \tilde{\mathrm{a}}\sin\frac{2\pi}{\lambda}(\tilde{\mathrm{x}}-\tilde{\mathrm{t}})\right], \tag{4.1}$$

The governing equation are:

$$\frac{\partial\bar{v}}{\partial\tilde{r}}+\frac{\tilde{R}}{\tilde{r}+\tilde{R}}\frac{\partial\tilde{u}}{\partial\tilde{x}}+\frac{\tilde{v}}{\tilde{r}+\tilde{R}}=0, \tag{4.2}$$

$$\rho\left[\frac{\partial\tilde{u}}{\partial\tilde{t}}+\tilde{v}\frac{\partial\bar{u}}{\partial\tilde{r}}+\frac{\tilde{R}}{\tilde{r}+\tilde{R}}\frac{\partial\tilde{u}}{\partial\tilde{x}}+\frac{\tilde{u}\tilde{v}}{\tilde{r}+\tilde{R}}\right]=\frac{1}{(\tilde{r}+\tilde{R})}\frac{\partial}{\partial\tilde{r}}\left\{(\tilde{r}+\tilde{R})^2\tilde{S}_{\tilde{r}\tilde{x}}\right\}+\frac{\tilde{R}}{\tilde{r}+\tilde{R}}\frac{\partial\tilde{S}_{\tilde{x}\tilde{x}}}{\partial\tilde{x}}-\frac{\tilde{R}}{\tilde{r}+\tilde{R}}\frac{\partial\tilde{p}}{\partial\tilde{x}}, \tag{4.3}$$

$$\rho\left[\frac{\partial\tilde{v}}{\partial\tilde{t}}+\tilde{v}\frac{\partial\tilde{v}}{\partial\tilde{r}}+\frac{\tilde{R}\tilde{u}}{\tilde{r}+\tilde{R}}\frac{\partial\tilde{v}}{\partial\tilde{x}}-\frac{\tilde{u}^2}{\tilde{r}+\tilde{R}}\right]=-\frac{\partial\tilde{p}}{\partial\tilde{r}}+\frac{1}{(\tilde{r}+\tilde{R})}\frac{\partial}{\partial\tilde{r}}\left\{(\tilde{r}+\tilde{R})\tilde{S}_{\tilde{r}\tilde{r}}\right\}+\frac{\tilde{R}}{\tilde{r}+\tilde{R}}\frac{\partial\tilde{S}_{\tilde{x}\tilde{r}}}{\partial\tilde{x}}-\frac{\tilde{S}_{\tilde{r}\tilde{x}}}{\tilde{r}+\tilde{R}}, \tag{4.4}$$

$$\rho c_p\left[\frac{\partial}{\partial\tilde{t}}+\tilde{v}\frac{\partial}{\partial\tilde{r}}+\frac{\tilde{R}\tilde{u}}{\tilde{r}+\tilde{R}}\frac{\partial}{\partial\tilde{x}}\right]\tilde{T}=\tilde{k}\left[\frac{\partial^2\tilde{T}}{\partial\tilde{r}^2}+\frac{1}{\tilde{r}+\tilde{R}}\frac{\partial}{\partial\tilde{r}}+\frac{\partial^2}{\partial\tilde{x}^2}\right]+\left(\tilde{S}_{\tilde{r}\tilde{r}}-\tilde{S}_{\tilde{x}\tilde{x}}\right)\frac{\partial\tilde{v}}{\partial\tilde{r}}+\tilde{S}_{\tilde{r}\tilde{x}}\left[\frac{\partial\tilde{u}}{\partial\tilde{r}}+\frac{\tilde{R}}{\tilde{r}+\tilde{R}}\frac{\partial\tilde{v}}{\partial\tilde{x}}-\frac{\tilde{u}}{\tilde{r}+\tilde{R}}\right], \tag{4.5}$$

With the following constitutive relation for pseudoplastic fluid

$$\tilde{\boldsymbol{S}}+\tilde{\lambda}_1\frac{D\tilde{\boldsymbol{S}}}{D\tilde{t}}+\frac{1}{2}\left(\tilde{\lambda}_1+\tilde{\mu}_1\right)\left(\widetilde{\boldsymbol{A}}_1\tilde{\boldsymbol{S}}+\tilde{\boldsymbol{S}}\widetilde{\boldsymbol{A}}_1\right)=\tilde{\mu}\widetilde{\boldsymbol{A}}_1,$$

$$\widetilde{\boldsymbol{A}}_1=grad\tilde{\boldsymbol{v}}+(grad\tilde{\boldsymbol{v}})^T,$$

$$\frac{D\tilde{\boldsymbol{S}}}{D\tilde{t}}=\frac{d\tilde{\boldsymbol{S}}}{d\tilde{\boldsymbol{t}}}-(grad\tilde{\boldsymbol{v}})\tilde{\boldsymbol{S}}+\tilde{\boldsymbol{S}}(grad\tilde{\boldsymbol{v}})^T.$$

Here $\widetilde{\boldsymbol{A}}_1$ is a first rivlin Ericksen tensor, $\frac{D}{D\tilde{t}}$ represent total derivative with respect to time and $\frac{d}{d\tilde{t}}$ represent instantaneous derivative with respect to time.

In the equations that are given below, several parameters are defined: $\tilde{p}$ signifies pressure, $\tilde{\mu}$ symbolizes dynamic viscosity, ρ denotes fluid density, $\tilde{R}$ represents the curvature parameter, σ stands for elastic tension, $\tilde{\eta}$ is the coefficient of viscous damping, $\tilde{T}$ signifies fluid temperature, $\tilde{D}$ stands for mass diffusivity coefficient, $\tilde{K}\tilde{T}$ signifies thermal diffusion ratio, and c_p signifies the specific heat at constant volume. Additionally, $\tilde{T}_m$ refers to the mean flow temperature, $\tilde{\mu}_1$ and $\tilde{\lambda}_1$ represent relaxation times for the pseudoplastic liquid, and $\tilde{S}_{\tilde{r}\tilde{x}}$, $\tilde{S}_{\tilde{r}\tilde{r}}$ and $\tilde{S}_{\tilde{x}\tilde{x}}$ pertain to components of the additional stress tensor $\tilde{S}$.

The components of the extra stress tensor are

$$\left[\tilde{S}_{\tilde{r}\tilde{r}}+\tilde{\lambda}_1\left\{\left(\frac{\partial}{\partial\tilde{t}}+\tilde{v}\frac{\partial}{\partial\tilde{r}}+\frac{\tilde{R}\tilde{u}}{\tilde{r}+\tilde{R}}\frac{\partial}{\partial\tilde{x}}\right)\tilde{S}_{\tilde{r}\tilde{r}}-2\tilde{S}_{\tilde{r}\tilde{r}}\frac{\partial\tilde{v}}{\partial\tilde{x}}-\frac{2\tilde{R}\tilde{u}}{\tilde{r}+\tilde{R}}\frac{\partial\tilde{v}}{\partial\tilde{x}}\right\}+\frac{1}{2}\left(\tilde{\lambda}_1-\tilde{\mu}_1\right)\left\{4\tilde{S}_{\tilde{r}\tilde{r}}\frac{\partial\tilde{v}}{\partial\tilde{r}}+2\tilde{S}_{\tilde{r}\tilde{x}}\left(\frac{\partial\tilde{u}}{\partial\tilde{r}}-\frac{\tilde{u}}{\tilde{r}+\tilde{R}}+\frac{\tilde{R}}{\tilde{r}+\tilde{R}}\frac{\partial\tilde{v}}{\partial\tilde{x}}\right)\right\}\right]=2\tilde{\mu}\frac{\partial\tilde{v}}{\partial\tilde{r}}, \tag{4.6}$$

$$\left[\tilde{S}_{\tilde{r}\tilde{x}}+\frac{1}{2}\left(\tilde{\lambda}_1-\tilde{\mu}_1\right)\left(\tilde{S}_{\tilde{r}\tilde{r}}+\tilde{S}_{\tilde{x}\tilde{x}}\right)\left(\frac{\partial\tilde{u}}{\partial\tilde{r}}-\frac{\tilde{u}}{\tilde{r}+\tilde{R}}+\frac{\tilde{R}}{\tilde{r}+\tilde{R}}\frac{\partial\tilde{v}}{\partial\tilde{x}}\right)+\tilde{\lambda}_1\left\{\left(\frac{\partial}{\partial\tilde{t}}+\tilde{v}\frac{\partial}{\partial\tilde{r}}+\frac{\tilde{R}\tilde{u}}{\tilde{r}+\tilde{R}}\frac{\partial}{\partial\tilde{x}}\right)\tilde{S}_{\tilde{r}\tilde{x}}-\tilde{S}_{\tilde{r}\tilde{r}}\left(\frac{\partial\tilde{u}}{\partial\tilde{r}}-\frac{\tilde{u}}{\tilde{r}+\tilde{R}}\right)-\frac{\tilde{R}\tilde{S}_{\tilde{x}\tilde{x}}}{\tilde{r}+\tilde{R}}\frac{\partial\tilde{v}}{\partial\tilde{x}}\right\}\right]=\tilde{\mu}\left(\frac{\partial\tilde{u}}{\partial\tilde{r}}-\frac{\tilde{u}}{\tilde{r}+\tilde{R}}+\frac{\tilde{R}}{\tilde{r}+\tilde{R}}\frac{\partial\tilde{v}}{\partial\tilde{x}}\right), \tag{4.7}$$

$$\left[\tilde{S}_{\tilde{x}\tilde{x}}+\frac{1}{2}\left(\tilde{\lambda}_1-\tilde{\mu}_1\right)\left\{\left(2\tilde{S}_{\tilde{r}\tilde{x}}\right)\left(\frac{\partial\tilde{u}}{\partial\tilde{r}}-\frac{\tilde{u}}{\tilde{r}+\tilde{R}}+\frac{\tilde{R}}{\tilde{r}+\tilde{R}}\frac{\partial\tilde{v}}{\partial\tilde{x}}\right)+4\tilde{S}_{\tilde{x}\tilde{x}}\left(\frac{\tilde{v}}{\tilde{r}+\tilde{R}}+\frac{\tilde{R}}{\tilde{r}+\tilde{R}}\frac{\partial\tilde{u}}{\partial\tilde{x}}\right)\right\}+\tilde{\lambda}_1\left\{\left(\frac{\partial}{\partial\tilde{t}}+\tilde{v}\frac{\partial}{\partial\tilde{r}}+\frac{\tilde{R}\tilde{u}}{\tilde{r}+\tilde{R}}\frac{\partial}{\partial\tilde{x}}\right)\tilde{S}_{\tilde{x}\tilde{x}}-2\tilde{S}_{\tilde{r}\tilde{x}}\left(\frac{\partial\tilde{u}}{\partial\tilde{r}}-\frac{\tilde{u}}{\tilde{r}+\tilde{R}}\right)-2\tilde{S}_{\tilde{x}\tilde{x}}\left(\frac{\tilde{v}}{\tilde{r}+\tilde{R}}+\frac{\tilde{R}}{\tilde{r}+\tilde{R}}\frac{\partial\tilde{u}}{\partial\tilde{x}}\right)\right\}\right]=2\tilde{\mu}\left(\frac{\tilde{v}}{\tilde{r}+\tilde{R}}+\frac{\tilde{R}}{\tilde{r}+\tilde{R}}\frac{\partial\tilde{u}}{\partial\tilde{x}}\right), \tag{4.8}$$

The following boundary conditions are applied to the current problem:

$$\tilde{u}=0\,,\quad \tilde{T}=\begin{Bmatrix}\tilde{T}_1\\ \tilde{T}_2\end{Bmatrix},\qquad \text{at } \tilde{r}=\pm\tilde{\eta}, \tag{4.9}$$

$$\tilde{R}\left[-\tau\frac{\partial^3}{\partial\tilde{x}^3}+m\frac{\partial^3}{\partial\tilde{x}\partial\tilde{t}^2}+\frac{\partial^2}{\partial\tilde{x}\partial\tilde{t}}\right]\tilde{\eta}=\frac{1}{\tilde{r}+\tilde{R}}\frac{\partial}{\partial\tilde{r}}\left\{(\tilde{r}+\tilde{R})^2\tilde{S}_{\tilde{r}\tilde{x}}\right\}+\frac{\partial\tilde{S}_{\tilde{x}\tilde{x}}}{\partial\tilde{x}}-\rho(\tilde{r}+\tilde{R})\left[\frac{\partial\tilde{u}}{\partial\tilde{t}}+\tilde{v}\frac{\partial\bar{u}}{\partial\tilde{r}}+\frac{\tilde{R}}{\tilde{r}+\tilde{R}}\frac{\partial\tilde{u}}{\partial\tilde{x}}+\frac{\tilde{u}\tilde{v}}{\tilde{r}+\tilde{R}}\right]. \tag{4.10}$$

The initial boundary condition enforces the no-slip requirement at the walls, with $\tilde{T}_0$ representing the temperature at the lower walls, and $\tilde{T}_1$ denoting the temperature at the upper wall, respectively.

To simplify the analysis, we introduce the following dimensionless variables [68]:

$$u^*=\frac{\tilde{u}}{\tilde{c}},\ v^*=\frac{\tilde{v}}{\tilde{c}},\quad x^*=\frac{\tilde{x}}{\tilde{\lambda}},\quad r^*=\frac{\tilde{r}}{\tilde{d}_1},\quad t^*=\frac{\tilde{c}\tilde{t}}{\tilde{\lambda}},\quad \eta^*=\frac{\tilde{\eta}}{\tilde{d}_1}\quad \theta^*=\frac{\tilde{T}-\tilde{T}_0}{\tilde{T}_1-\tilde{T}_0},$$

$$p^*=\frac{\tilde{d}_1^2\tilde{p}}{\tilde{c}\tilde{\lambda}\tilde{\mu}},\quad S_{ij}^*=\frac{d_1\tilde{S}_{ij}}{\tilde{c}\tilde{\mu}},\quad \lambda_1^*=\frac{\tilde{\lambda}_1\tilde{c}}{\tilde{d}_1},\quad \mu_1^*=\frac{\tilde{\mu}_1\tilde{c}}{\tilde{d}_1}\quad k^*=\frac{\tilde{R}}{\tilde{d}_1}.$$

After using these dimension less variable and ignoring' * 'the system of equations from (4.3) to (4.10) becomes

$$\left[\frac{1}{2}(\lambda_1-\mu_1)\left\{4S_{rr}\frac{\partial v}{\partial r}+2S_{rx}\left(\frac{\partial u}{\partial r}-\frac{u}{r+k}+\frac{k\delta}{r+k}\frac{\partial v}{\partial x}\right)\right\}+S_{rr}+\lambda_1\left\{\left(\delta\frac{\partial}{\partial t}+v\frac{\partial}{\partial r}+\frac{k\delta u}{r+k}\frac{\partial}{\partial x}\right)S_{rr}-2S_{rr}\frac{\partial v}{\partial r}-\frac{2k\delta u}{r+k}\frac{\partial v}{\partial x}\right\}\right]=2\frac{\partial v}{\partial r}, \tag{4.11}$$

$$\left[\lambda_1\left\{\left(\delta\frac{\partial}{\partial t}+v\frac{\partial}{\partial r}+\frac{k\delta u}{r+k}\frac{\partial}{\partial x}\right)S_{rx}-S_{rr}\left(\frac{\partial u}{\partial r}-\frac{u}{r+k}\right)-\frac{k\delta S_{xx}}{r+k}\frac{\partial v}{\partial x}\right\}+S_{rx}+\frac{1}{2}(\lambda_1-\mu_1)(S_{rr}+S_{xx})\left(\frac{\partial u}{\partial r}-\frac{u}{r+k}+\frac{k\delta}{r+k}\frac{\partial v}{\partial x}\right)\right]=\left(\frac{\partial u}{\partial r}-\frac{u}{r+k}+\frac{k\delta}{r+k}\frac{\partial v}{\partial x}\right), \tag{4.12}$$

$$\left[\lambda_1\left\{\left(\delta\frac{\partial}{\partial t}+v\frac{\partial}{\partial r}+\frac{k\delta u}{r+k}\frac{\partial}{\partial x}\right)S_{xx}-2S_{rx}\left(\frac{\partial u}{\partial r}-\frac{u}{r+k}\right)-2S_{xx}\left(\frac{v}{r+k}+\frac{R}{r+k}\frac{\partial u}{\partial x}\right)\right\}+S_{xx}+\frac{1}{2}(\lambda_1-\mu_1)\left\{(2S_{rx})\left(\frac{\partial u}{\partial r}-\frac{u}{r+k}+\frac{k\delta}{r+k}\frac{\partial v}{\partial x}\right)+4S_{xx}\left(\frac{v}{r+k}+\frac{u\delta}{r+k}\frac{\partial u}{\partial x}\right)\right\}\right]=2\left(\frac{v}{r+k}+\frac{u\delta}{r+k}\frac{\partial u}{\partial x}\right), \tag{4.13}$$

$$Re\delta\left[\delta\frac{\partial v}{\partial t}+\ v\frac{\partial v}{\partial r}\ +\ \frac{k\delta u}{r+k}\frac{\partial v}{\partial x}-\frac{u^2}{r+k}\right]=\delta\left[\frac{1}{r+k}\frac{\partial}{\partial r}\{(r+k)S_{rr}\}+\frac{k\delta}{r+k}\frac{\partial S_{rx}}{\partial x}-\frac{S_{xx}}{r+k}\right]-\frac{\partial p}{\partial r},\quad (4.14)$$

$$Re\left[\delta\frac{\partial u}{\partial t}+\ v\frac{\partial u}{\partial r}\ +\ \frac{k\delta u}{r+k}\frac{\partial u}{\partial x}+\frac{uv}{r+k}\right]=\frac{k\delta}{r+k}\frac{\partial S_{xx}}{\partial x}-\frac{k}{r+k}\frac{\partial p}{\partial x}+\frac{1}{(r+k)^2}\frac{\partial}{\partial r}\{(r+k)^2S_{rx}\},\quad (4.15)$$

$$Re\left[\delta\frac{\partial}{\partial t}+\ v\frac{\partial}{\partial r}\ +\ \frac{k\delta u}{r+k}\frac{\partial u}{\partial x}\right]\theta=Ec\left[(S_{rr}-S_{xx})\frac{\partial v}{\partial r}+S_{rx}\left[\frac{\partial u}{\partial r}-\frac{u}{r+k}+\frac{k\delta}{r+k}\frac{\partial v}{\partial x}\right]\right]+\frac{1}{Pr}\left[\frac{\partial^2}{\partial r^2}+\frac{1}{r+k}\frac{\partial}{\partial r}+\ \delta^2\frac{\partial^2}{\partial x^2}\right]\theta\ ,\quad (4.16)$$

With boundary conditions:

$$u=0,\ \theta=\begin{Bmatrix}1\\0\end{Bmatrix},\ at\ r=\pm\eta=\pm\big(1+\epsilon sin2\pi(x-t)\big),\quad (4.17)$$

$$k\left[E_1\frac{\partial^3}{\partial x^3}+E_2\frac{\partial^3}{\partial x\partial t^2}+E_3\frac{\partial^2}{\partial x\partial t}\right]\eta=\delta\frac{\partial S_{xx}}{\partial x}+\frac{1}{r+k}\frac{\partial}{\partial r}\{(r+k)^2S_{rx}\}-Re(r+k)\ \left[\delta\frac{\partial u}{\partial t}+\ v\frac{\partial u}{\partial r}\ +\ \frac{k\delta u}{r+k}\frac{\partial u}{\partial x}+\frac{uv}{r+k}\right].\quad (4.18)$$

Here, dimensionless parameter is k, Eckert number is equal to $Ec=\frac{c^2}{(T_1-T_0)C_P}$, amplitude ratio $\epsilon=\frac{a}{d_1}$, Reynolds number $Re=\ \frac{d_1c}{v}$, the Schmidt number is $Sc=\ \frac{\mu}{\rho D}$, Wave number is $\delta=\frac{d_1}{\lambda}$, Wall tension is equal to $E_1=\frac{-\tau d_1^3}{\lambda^3\mu}$, wall damping parameter is equal to $E_3=\frac{d_1^3}{\lambda^2\mu}$, mass characterizing parameter is $E_2=\frac{mcd_1^3}{\lambda^3\mu}$ and the brinkman number is equal to $Br\ =\ EcPr$.

Introducing stream function $\psi(x,y,t)$ one can express as

$$u=-\frac{\partial\psi}{\partial r},\qquad v=\frac{k\delta}{r+k}\frac{\partial\psi}{\partial x}.$$

After applying long wavelength and low Reynolds number assumptions, we obtain the following equations.

$$\frac{\partial p}{\partial r}=0,\quad (4.19)$$

$$-\frac{k}{r+k}\frac{\partial p}{\partial x}+\frac{1}{(r+k)^2}\frac{\partial}{\partial r}\{(r+k)^2S_{rx}\}\ \ =0,\quad (4.20)$$

$$\left[\frac{\partial^2}{\partial r^2}+\frac{1}{r+k}\frac{\partial}{\partial r}\right]\theta=-Br\left[S_{rx}\left(\frac{\psi_r}{r+k}-\psi_{rr}\right)\right],\quad (4.21)$$

$$\psi_r=0\ ,\qquad \theta=\begin{Bmatrix}1\\0\end{Bmatrix},\qquad \text{at}\ \ r=\pm\eta=\pm\big(1+\epsilon sin2\pi(x-t)\big),\quad (4.22)$$

$$k\left[E_1\frac{\partial^3}{\partial x^3}+E_2\frac{\partial^3}{\partial x\partial t^2}+E_3\frac{\partial^2}{\partial x\partial t}\right]\eta=\frac{1}{r+k}\frac{\partial}{\partial r}\{(r+k)^2S_{rx}\},\ \text{at}\ r=\pm\eta,\quad (4.23)$$

with

$$S_{rr}+\ \ (\lambda_1-\mu_1)S_{rx}\left(\frac{\psi_r}{r+k}-\psi_{rr}\right)=0,\quad (4.24)$$

$$S_{rx}+\frac{1}{2}(\lambda_1-\mu_1)(S_{rr}+S_{xx})\left(\frac{\psi_r}{r+k}-\psi_{rr}\right)-\lambda_1S_{rr}\left(\frac{\psi_r}{r+k}-\psi_{rr}\right)=\left(\frac{\psi_r}{r+k}-\psi_{rr}\right),\quad (4.25)$$

$$S_{xx} + 2\lambda_1 S_{rx}\left(\frac{\psi_r}{r+k} - \psi_{rr}\right) + (\lambda_1 - \mu_1) S_{rx}\left(\frac{\psi_r}{r+k} - \psi_{rr}\right) = 0, \quad (4.26)$$

Combining equations (4.19) - (4.20) and (4.24) - (4.26), we get

$$\frac{\partial}{\partial r}\left[\frac{1}{k(r+k)}\frac{\partial}{\partial r}\{(r+k)^2 S_{rx}\}\right] = 0, \quad (4.27)$$

$$S_{rx} = \left(\frac{\psi_r}{r+k} - \psi_{rr}\right)\left[1 - \xi\left(\frac{\psi_r}{r+k} - \psi_{rr}\right)^2\right]^{-1}, \quad (4.28)$$

where $\xi = (\mu_1^2 - \lambda_1^2)$ is the pseudoplastic fluid parameter.

4.3 Method of solution

Using the small parameter ξ, we open the perturbation series provided below:

$$\psi = \psi_0 + \xi\psi_1 + \cdots \quad (4.29)$$

$$S_{rx} = S_{0rx} + \xi S_{1rx} + \cdots \quad (4.30)$$

$$\theta = \theta_0 + \xi\theta_1 + \cdots \quad (4.31)$$

4.3.1 Zero order system

Putting above expression in equations (4.20)-(4.23), then comparing the coefficient of ξ^0 , we get

$$\frac{\partial}{\partial r}\frac{1}{k(r+k)}\frac{\partial}{\partial r}\{(r+k)^2 S_{0rx}\} = 0, \quad (4.32)$$

$$\left[\frac{\partial^2}{\partial r^2} + \frac{1}{r+k}\frac{\partial}{\partial r}\right]\theta_0 = -Br\left[S_{0rx}\left(\frac{\psi_{0r}}{r+k} - \psi_{0rr}\right)\right], \quad (4.33)$$

$$\psi_{0r} = 0\,, \quad \theta_0 = \begin{Bmatrix}1\\0\end{Bmatrix}, \quad \text{at } r = \pm\eta, \quad (4.34)$$

$$k\left[E_1\frac{\partial^3}{\partial x^3} + E_2\frac{\partial^3}{\partial x\partial t^2} + E_3\frac{\partial^2}{\partial x\partial t}\right]\eta = \frac{1}{r+k}\frac{\partial}{\partial \bar{r}}\{(r+k)^2 S_{0rx}\}, \text{ at } r = \pm\eta, \quad (4.35)$$

$$S_{0rx} = \frac{\psi_r}{r+k} - \psi_{rr}\,.$$

The solution of the above-mentioned system is given as:

$$\psi_0 = \tilde{C}_1 + \tilde{C}_2\, ln(r+k) + \tilde{C}_3\, ln(r+k)^2 + \tilde{C}_4(r+k)\, ln(r+k)^2, \quad (4.36)$$

$$u_0 = -\psi_{0r} = -\frac{\tilde{C}_2}{r+k} - 2\tilde{C}_3(r+k) - \tilde{C}_4(r+k)\{1 + 2\, ln(r+k)\}\,, \quad (4.37)$$

$$\theta_0 = \tilde{A}_1 + \tilde{A}_2\, ln(r+k) + 4Br\tilde{C}_2\tilde{C}_4\, ln(r+k)^2 - Br\tilde{C}_4^2(r+k)^2 + \frac{\tilde{C}_2^2}{(r+k)^2}\,, \quad (4.38)$$

$$\tilde{\mathrm{C}}_1 = -\tilde{\mathrm{C}}_2 ln\mathrm{k} - \tilde{\mathrm{C}}_3 ln\mathrm{k}^2 - \tilde{\mathrm{C}}_4 k^2 ln\mathrm{k}\,,$$

$\tilde{C}_2 = \frac{\tilde{C}_4}{2k\eta}(-\eta^2 + k^2)^2 ln\left(\frac{\eta+k}{-\eta+k}\right)$,

$\tilde{C}_3 = -\frac{\tilde{C}_4}{4k\eta}(2k\eta + (\eta + k)^2 ln(\eta + k) - (-\eta + k)^2 ln(-\eta + k))$,

$\tilde{C}_4 = -2\epsilon\pi^3 k\left\{\frac{\tilde{E}_3}{2\pi} sin2\pi(x - t) - (E_1 + E_2)cos2\pi(x - t)\right\}$,

$\tilde{L}_1 = 1 + 4Br\left[\frac{\tilde{C}_4^2(\eta+k)^2}{4} + \frac{\tilde{C}_2^2}{4(\eta+k)^2} - \tilde{C}_2\tilde{C}_4(\ln(\eta + k))^2\right]$,

$\tilde{L}_2 = 4Br\left[\frac{\tilde{C}_4^2(-\eta+k)^2}{4} + \frac{\tilde{C}_2^2}{4(-\eta+k)^2} - \tilde{C}_2\tilde{C}_4(\ln(-\eta + k))^2\right]$,

$\widetilde{A}_2 = \frac{L_1+L_2}{\ln(\eta+k)-\ln(-\eta+k)}$.

4.3.2 First order system

The first order system is:

$$\frac{\partial}{\partial r}\frac{1}{k(r+k)}\frac{\partial}{\partial r}\{(r + k)^2 S_{1rx}\} = 0, \tag{4.39}$$

$$\left[\frac{\partial^2}{\partial r^2} + \frac{1}{r+k}\frac{\partial}{\partial r}\right]\theta_0 = -Br\left[S_{1rx}\left(\frac{\psi_{1r}}{r+k} - \psi_{1rr}\right) + S_{1rx}\left(\frac{\psi_{0r}}{r+k} - \psi_{0rr}\right)\right], \tag{4.40}$$

$$\psi_{1r} = 0\ , \quad \theta_1 = \begin{Bmatrix}1\\0\end{Bmatrix}, \quad \text{at } r = \pm\eta, \tag{4.41}$$

$$\frac{1}{(r+k)}\frac{\partial}{\partial r}\{(r + k)^2 S_{1rx}\} = 0, \text{ at } \quad r = \pm\eta, \tag{4.42}$$

$S_{1rx} = \frac{\psi_{1r}}{r+k} - \psi_{1rr} - \left(\frac{\psi_{0r}}{r+k} - \psi_{0rr}\right)^3$.

Using the zero order system into first order system and then solving the resulting problem, one arrives at following results:

$\psi_1 = \tilde{C}_{11} + \tilde{C}_{12}\ln(r + k) + \tilde{C}_{13}(r + k)^2 + \tilde{C}_{14}(r + k)^2\ln(r + k) - \frac{3\tilde{C}_2^2\tilde{C}_4}{(r+k)^2} + \frac{\tilde{C}_2^3}{3(r+k)^4}$,

$u_1 = -\psi_1'[r] = -\frac{\tilde{C}_{12}}{r+k} - 2\tilde{C}_{13}(r + k) - \tilde{C}_{14}(r + k)(1 + 2(r + k)) - \frac{6\tilde{C}_2^2\tilde{C}_4}{(r+k)^3} + \frac{4\tilde{C}_2^3}{3(r+k)^5}$,

$\theta_1 = \widetilde{A}_{11} + \widetilde{A}_{12} ln(r + k) + \frac{i_1(r+k)^2}{4} + \frac{i_2(ln(r+k))^2}{2} + \frac{i_3}{4(r+k)^2} + \frac{i_4}{16(r+k)^4} + \frac{i_5}{36(r+k)^6}$,

where,

$\tilde{C}_{11} = -\tilde{C}_{12} ln(k) - \tilde{C}_{13}(k)^2 - \tilde{C}_{14}(k)^2 ln(k) + \frac{3\tilde{C}_2{}^2\tilde{C}_4}{(k)^2} - \frac{\tilde{C}_2{}^3}{3(k)^4}$,

$\tilde{C}_{12} = \frac{-(k^2-\eta^2)}{4k\eta}((-\eta + k)\widetilde{B}_1 - (\eta + k)\widetilde{B}_2)$,

$\tilde{C}_{13} = \frac{1}{8k\eta}\left((\eta + k)\widetilde{B}_1 - (-\eta + k)\widetilde{B}_2\right)$,

$\tilde{\mathrm{C}}_{14} = -4\tilde{C}_4^3$,

$\tilde{\mathrm{B}}_1 = -\tilde{\mathrm{C}}_{14}(\eta + k)(1 + 2\ln(\eta + k)) - \tilde{C}_2^2\left(\frac{6\tilde{\mathrm{C}}_4}{(\eta+k)^3} - \frac{4\tilde{\mathrm{C}}_2}{3(\eta+k)^5}\right)$,

$\tilde{\mathrm{B}}_2 = -\tilde{\mathrm{C}}_{14}(-\eta + k)(1 + 2\ln(-\eta + k)) - \tilde{C}_2^2\left(\frac{6\tilde{\mathrm{C}}_4}{(-\eta+k)^3} - \frac{4\tilde{\mathrm{C}}_2}{3(-\eta+k)^5}\right)$,

$\tilde{A}_{11} = \frac{L_3 ln(\eta+k) - L_4 ln(\eta+k)}{ln(\eta+k) - ln(\eta+k)}$,

$\tilde{A}_{12} = \frac{\tilde{L}_3 - L_4}{ln(\eta+k) - ln(\eta+k)}$,

$\tilde{L}_3 = -\left[\frac{i_1(\eta+k)^2}{4} + \frac{i_2(ln(\eta+k))^2}{2} + \frac{i_3}{4(\eta+k)^2} + \frac{i_4}{16(\eta+k)^4} + \frac{i_5}{36(\eta+k)^6}\right]$,

$\tilde{L}_4 = -\left[\frac{i_1(-\eta+k)^2}{4} + \frac{i_2(ln(-\eta+k))^2}{2} + \frac{i_3}{4(-\eta+k)^2} + \frac{i_4}{16(-\eta+k)^4} + \frac{i_5}{36(-\eta+k)^6}\right]$,

$i_1 = -2Br\tilde{C}_4(4\tilde{C}_{14} + 8\tilde{C}_4^3)$,

$i_2 = 2Br\left(4\tilde{C}_2\tilde{C}_{14} + 4\tilde{C}_4\tilde{C}_{12} + 32\tilde{C}_2\tilde{C}_4^3\right)$,

$i_3 = -8Br\tilde{C}_2\tilde{C}_{12}$,

$i_4 = -64\tilde{C}_4\tilde{C}_2^3$,

$i_5 = 16Br\tilde{C}_2^4$.

To see the impact of the parameters like E_1, E_2 and E_3, the curvature co-efficient ' k ' and the pseudoplastic parameter ξ , the graphs for velocity, streamlines and temperature are plotted by using the MATHIMATICA software.

4.4 Result and discussion

This section contains the physical interpretation of the obtained results through Figs 4.2 to 4.8 The values of ξ , Br and E_i characterise the strengths of shear-thinning, viscous dissipation and elasticity effects respectively. Understanding these parameters is crucial for interpreting the results. ξ characterizes shear-thinning, where viscosity decreases with higher shear rates. A higher ξ signifies a more pronounced shear-thinning effect, indicating that the material becomes less viscous and flows more readily as shear rates increase. This parameter indicates the material's sensitivity to shear rate changes, with a larger ξ indicating a stronger response. Br relates to viscous dissipation, representing the energy loss due to internal friction or viscosity within the material. E_i $(i = 1,2,3)$ represents elasticity effects. A higher Br value signifies a heightened viscous dissipation effect within the system, indicating substantial energy dissipation due to viscosity. This leads to heating or a loss of mechanical energy during deformation. Elasticity in a material pertains to its ability to revert to its original shape after

deformation. A higher E_i $(i = 1,2,3)$ value indicates a more pronounced elasticity effect, signifying the material's strong tendency to regain its initial shape once the deforming force is removed. A larger E_i $(i = 1,2,3)$value suggests a higher level of elasticity, allowing the material to store and release more energy during deformation. Larger ξ values denote a more prominent shear-thinning effect, larger Br values indicate a stronger viscous dissipation effect, and larger E_i $(i = 1,2,3)$values represent a more significant elasticity effect. Fig. 4.2 illustrates how the axial velocity deviates as the material fluid parameter ξ varies. As ξ increases, it signifies a rise in the shear-thickening effect or, in other words, an increase in fluid viscosity as the rate of deformation intensifies. This heightened viscosity opposes the flow, resulting in a reduction in velocity. This behavior is also observed in a planar channel. Unlike the curved channel, the axial velocity profiles in the planar channel display symmetry around the central line. Fig. 4.3 illustrates velocity profiles associated with varying elasticity parameters: E_1, E_2, and E_3. It is observed that the axial velocity exhibits a positive correlation with E_1. In terms of physics, an increase in E_1 alleviates tension in the blood vessel walls, resulting in an acceleration of blood flow. Furthermore, the velocity escalates with an augmentation in the wall mass per unit area. For elevated values of E_3, the walls of the channel (or blood vessels) experience heightened damping effects. Under such conditions, the arteries or blood vessels necessitate a more significant force to expand and accommodate the blood ejected from the heart. This subsequently leads to a reduction in the blood velocity inside the vessels. Fig. 4.4 illustrates that as the Brinkman number (Br) is elevated, there is a corresponding increase in temperature (θ). This phenomenon can be attributed to the higher values of Br indicating more pronounced viscous dissipation, leading to increased heat generation from friction resulting from shear within the flow. As a consequence, the fluid temperature rises. The temperature profiles exhibit maxima in proximity to the upper wall of the curved channel. Fig. 4.5 clarifies how the curvature of the channel influences the distribution of temperature. It is observed that as the channel approaches a planar configuration, the temperature profiles symmetrically align around the central region.

In Fig. 4.6, the impact of the fluid parameter ξ on temperature distribution is observed. The analysis reveals that as the shear-thinning or shear-thickening effect intensifies, the temperature within the channel either rises or falls accordingly. Notably, the highest points in the temperature profiles are located in the vicinity of the upper wall, whether the channel is curved or planar. Additionally, it's worth mentioning that the temperature profiles lack symmetry around the central region, diverging from the symmetry observed in a planar channel.

Fig. 4.7 and Fig. 4.8 depict streamlines illustrating the influence of different parameters: curvature parameter k, fluid material parameter ξ, and elastic parameters E_1, E_2, and E_3.

In Fig. 4.7, it's evident that the size and quantity of trapped boluses increase as the curvature parameter k is raised, particularly in the upper half of the channel ($r > 0$). Conversely, in the lower half of the channel ($r < 0$), an increase in curvature parameter k results in a reduction in the size of the trapped boluses. However, for significantly large values of k, the size and circulation of the trapped boluses tend to be similar in both the upper and lower halves of the channel. Fig. 4.8 (a–c) demonstrate that the size of trapped boluses, in both the upper and lower halves of the channel, increases with an augmentation of the fluid parameter $\xi > 0$. Conversely, an opposite trend is observed when $\xi < 0$ is increased.

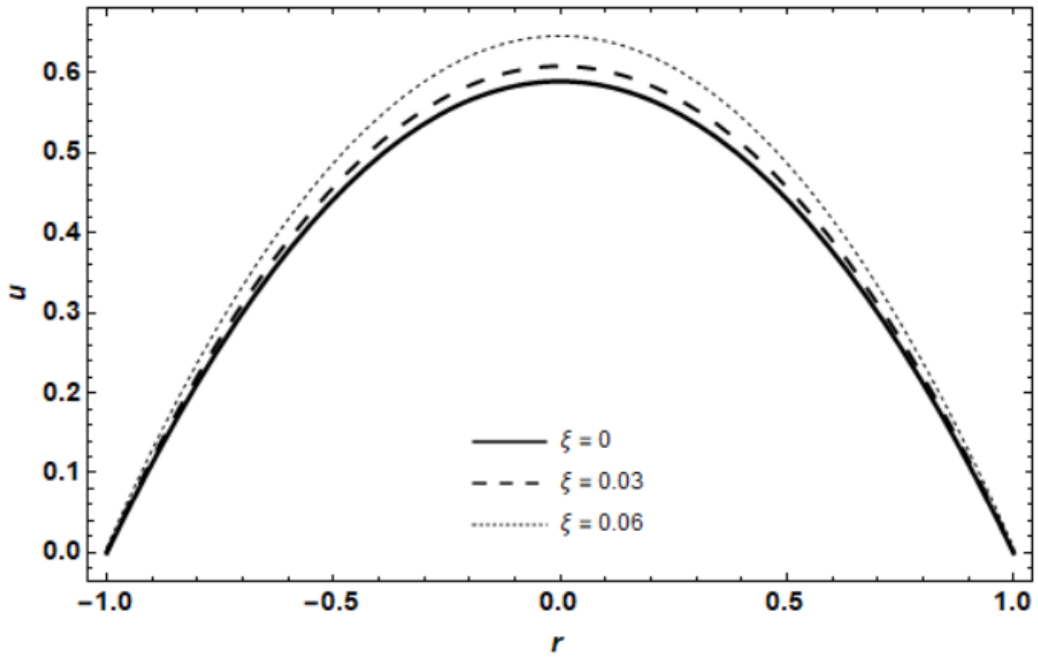

Fig 4.2: Variation of ξ on velocity of fluid 0, 0.03 and 0.06

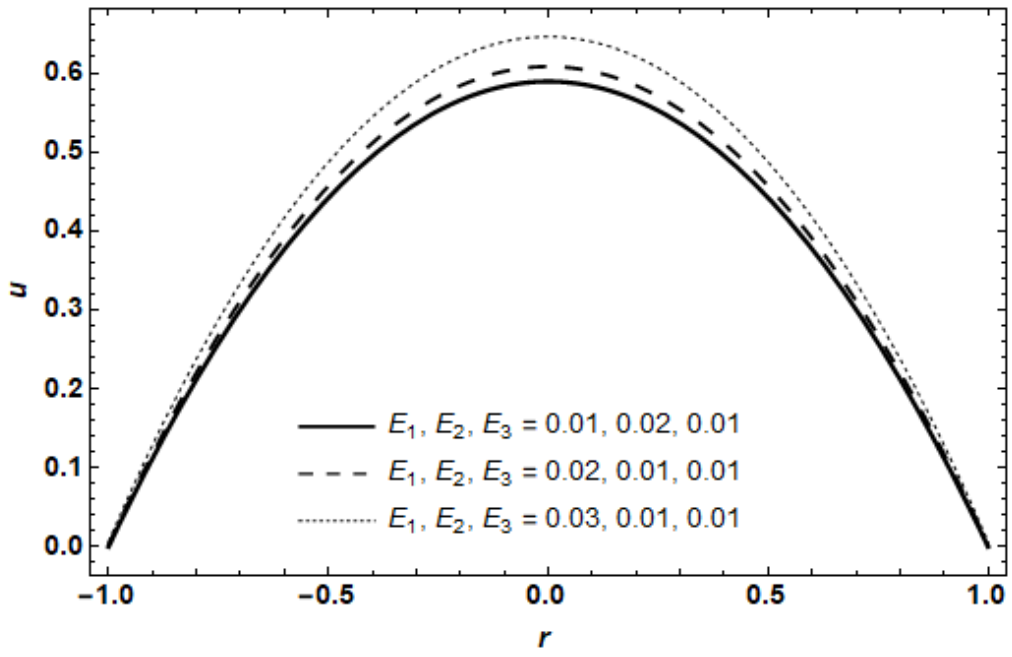

Fig 4.3: Variation of a complaint wall on a velocity of fluid.

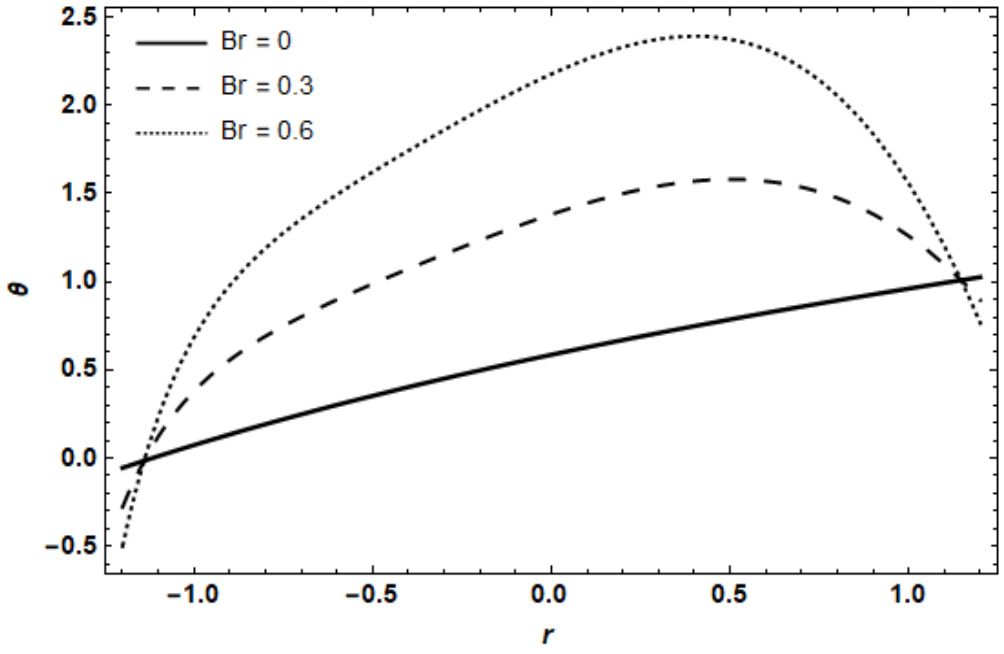

Fig 4.4: Variation of ***Br*** at 0, 0.3 and 0.6 on temperature of the fluid.

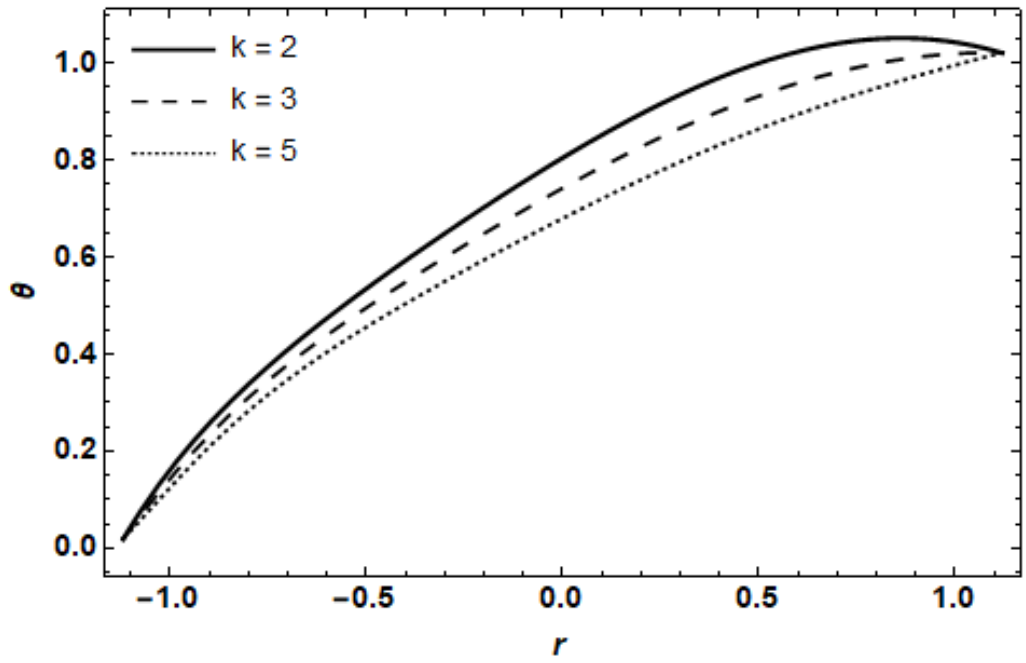

Fig 4.5: Variation of $\boldsymbol{k}$ on a temperature of the fluid at $\boldsymbol{k = 2, 3}$ and 5.

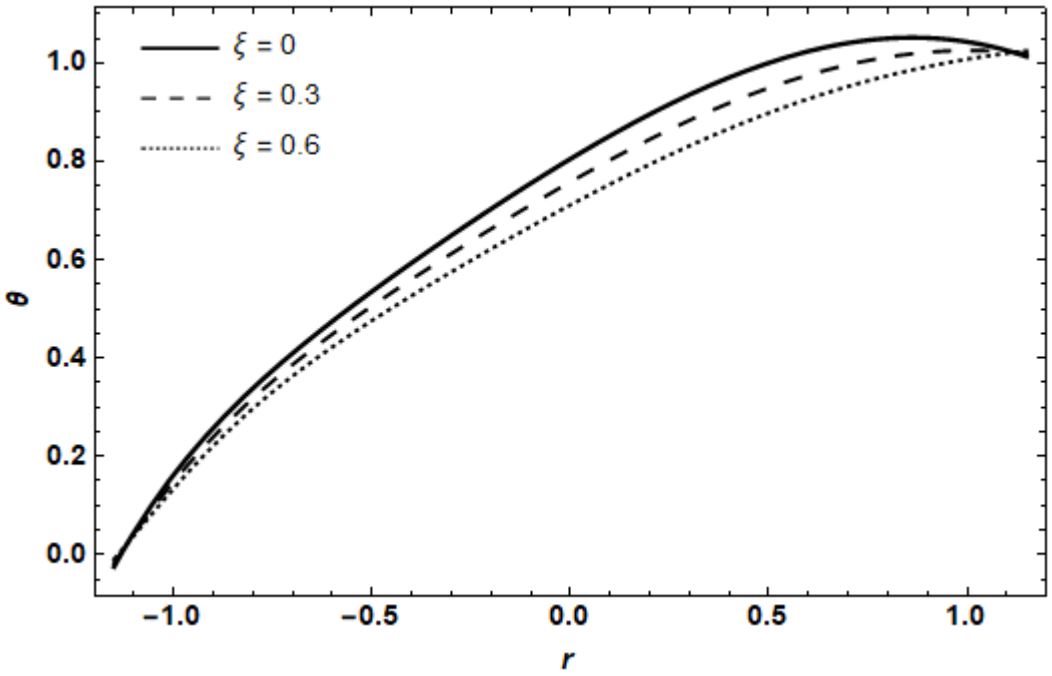

Fig 4.6: Variation of ξ at 0, 0.3 and 0.6 on a temperature of a fluid.

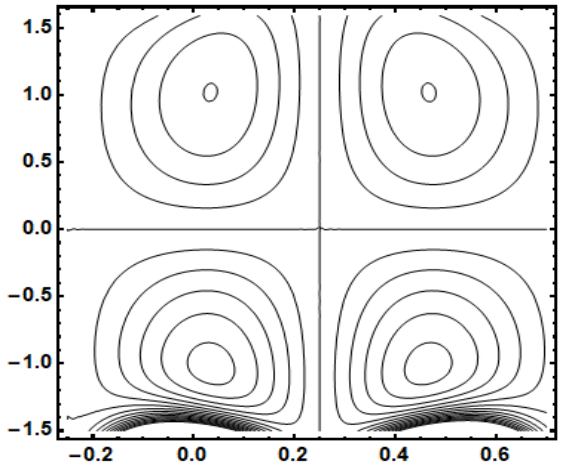

$(a)\ k\ =\ 2$

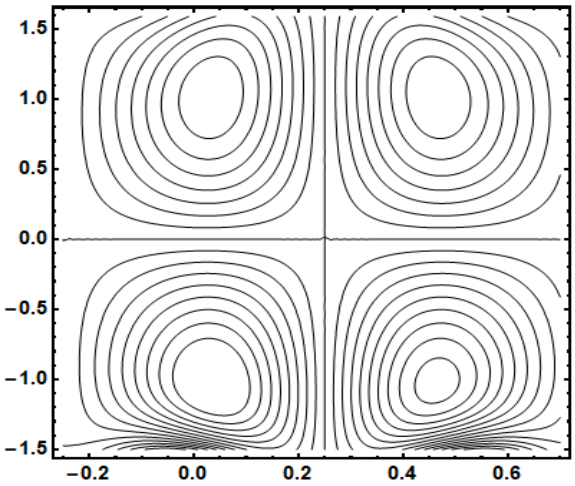

$(b)\ k\ =3$

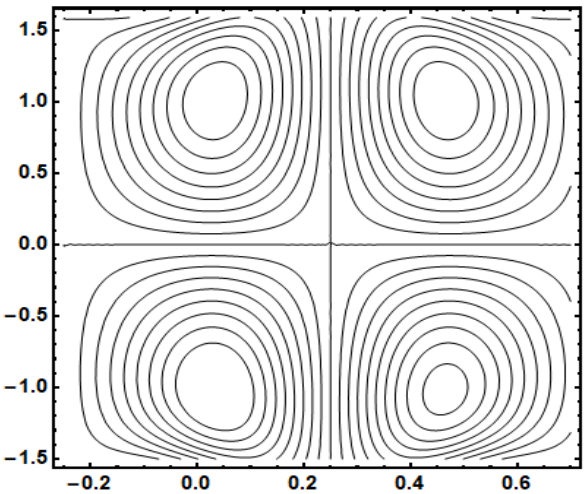

$(c)\ k \rightarrow \infty$

Fig 4.7: Variation of k on ψ at (a) $k = 2$ (b) $k = 3$ and (c) $k \rightarrow \infty$

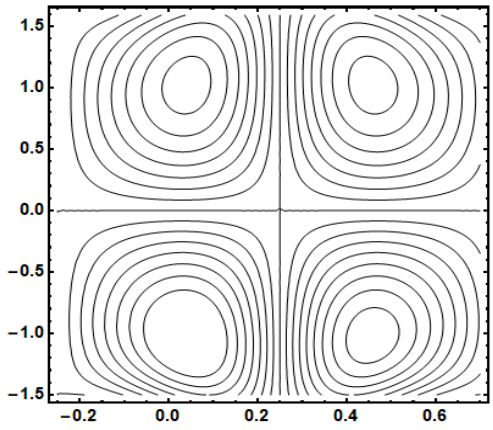

$(a)\ \xi = 0$

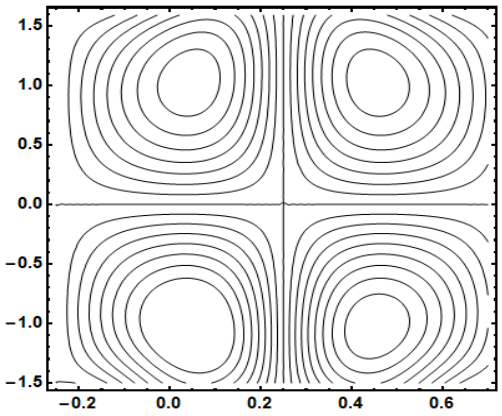

$(b)\ \xi = 0.0025$

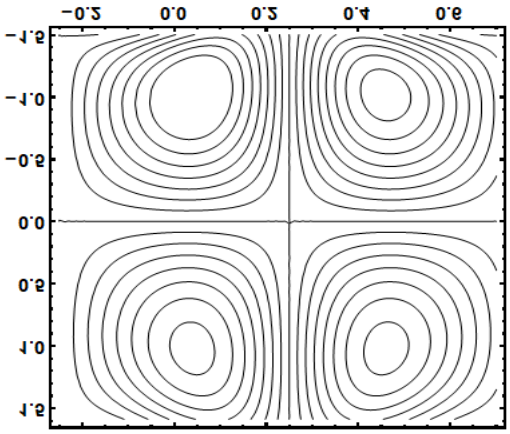

$(c)\ \xi = -0.0025$

Fig 4.8: Variation of ξ on ψ at (a) $\xi = 0$, (b) $\xi = 0.0025$ and (c) $\xi = -0.0025$

CHAPTER 5

INFLUENCE OF ENTROPY GENERATION ON PERISTALTIC TRANSPORT OF PSEUDOPLASTIC FLUID IN A CURVED CONFIGURATION

5.1 Introduction

In this chapter, we extended the work of Hina *et al*. [68] by investigating the entropy generation impact of peristaltic transport of pseudoplastic fluid in curved configuration along with MHD by assuming a long wavelength assumption. Also, we have applied perturbation techniques to solve PDE's and series solutions for stream function were derived**.** We have evaluated the suggested model by using Mathematica.

5.2 Mathematical formulation

In our extension work we are taking a curved channel with a thickness of $\tilde{d}_1$. The flow is characterized by a longitudinal axis denoted as x̃ and a radial path represented by r̃. The components of velocity in the longitudinal and peripheral directions are denoted as ũ and ṽ, respectively. The waves that are being propagated have a sinusoidal form, which may be described by equations.

$$\frac{\partial \tilde{v}}{\partial \tilde{r}} + \frac{\tilde{R}}{\tilde{r}+\tilde{R}}\frac{\partial \tilde{u}}{\partial \tilde{x}} + \frac{\tilde{v}}{\tilde{r}+\tilde{R}} = 0\,, \tag{5.1}$$

$$\rho\left[\frac{\partial \tilde{u}}{\partial \tilde{t}} + \tilde{v}\frac{\partial \tilde{u}}{\partial \tilde{r}} + \frac{\tilde{R}}{\tilde{r}+\tilde{R}}\frac{\partial \tilde{u}}{\partial \tilde{x}} + \frac{\tilde{u}\tilde{v}}{\tilde{r}+\tilde{R}}\right] = \frac{1}{(\tilde{r}+\tilde{R})}\frac{\partial}{\partial \tilde{r}}\left\{\left(\tilde{r}+\tilde{R}\right)^2\tilde{S}_{\tilde{r}\tilde{x}}\right\} + \frac{\tilde{R}}{\tilde{r}+\tilde{R}}\frac{\partial \tilde{S}_{\tilde{x}\tilde{x}}}{\partial \tilde{x}} - \frac{\tilde{R}}{\tilde{r}+\tilde{R}}\frac{\partial \tilde{p}}{\partial \tilde{x}} - \frac{\sigma B_0^2\tilde{u}}{(\tilde{r}+\tilde{R})^2}, \tag{5.2}$$

$$\rho\left[\frac{\partial \tilde{v}}{\partial \tilde{t}} + \tilde{v}\frac{\partial \tilde{v}}{\partial \tilde{r}} + \frac{\tilde{R}\tilde{u}}{\tilde{r}+\tilde{R}}\frac{\partial \tilde{v}}{\partial \tilde{x}} - \frac{\tilde{u}^2}{\tilde{r}+\tilde{R}}\right] = -\frac{\partial \tilde{p}}{\partial \tilde{r}} + \frac{1}{(\tilde{r}+\tilde{R})}\frac{\partial}{\partial \tilde{r}}\left\{\left(\tilde{r}+\tilde{R}\right)\tilde{S}_{\tilde{r}\tilde{r}}\right\} + \frac{\tilde{R}}{\tilde{r}+\tilde{R}}\frac{\partial \tilde{S}_{\tilde{x}\tilde{r}}}{\partial \tilde{x}} - \frac{\tilde{S}_{\tilde{r}\tilde{x}}}{\tilde{r}+\tilde{R}}. \tag{5.3}$$

In this chapter we are using the same tensor are utilized as discussed in chapter 4 mentioned in equation (4.6) - (4.8).

To simplify the analysis, we introduce the following dimensionless variables [68]:

$$u^* = \frac{\tilde{u}}{\tilde{c}},\ v^* = \frac{\tilde{v}}{\tilde{c}},\quad x^* = \frac{\tilde{x}}{\tilde{\lambda}},\quad r^* = \frac{\tilde{r}}{\tilde{d}_1},\quad t^* = \frac{\tilde{c}\tilde{t}}{\tilde{\lambda}},\quad \eta^* = \frac{\tilde{\eta}}{\tilde{d}_1}\quad \theta^* = \frac{\tilde{T}-\tilde{T}_0}{\tilde{T}_1-\tilde{T}_0},$$

$$p^* = \frac{\tilde{d}_1^2\,\tilde{p}}{\tilde{c}\tilde{\lambda}\tilde{\mu}},\quad S_{ij}^* = \frac{d_1\tilde{S}_{ij}}{\tilde{c}\tilde{\mu}},\quad \lambda_1^* = \frac{\tilde{\lambda}_1\tilde{c}}{\tilde{d}_1},\quad \mu_1^* = \frac{\tilde{\mu}_1\tilde{c}}{\tilde{d}_1}\quad k^* = \frac{\tilde{R}}{\tilde{d}_1}.$$

After putting dimension less variable the equations (5.3) are same as equation (4.14) and equation (5.2) is mentioned in equation (5.4).

$$Re\left[\delta\frac{\partial u}{\partial t} + v\frac{\partial u}{\partial r} + \frac{k\delta u}{r+k}\frac{\partial u}{\partial x} + \frac{uv}{r+k}\right] = \frac{k\delta}{r+k}\frac{\partial S_{xx}}{\partial x} - \frac{k}{r+k}\frac{\partial p}{\partial x} + \frac{1}{(r+k)^2}\frac{\partial}{\partial r}\{(r+k)^2 S_{rx}\} -$$

$$M^2\,\frac{\tilde{u}}{(\tilde{r}+\tilde{k})^2}, \tag{5.4}$$

The following boundary condition are applied to the current problem:

$$\psi = -\frac{F}{2},\ \psi = 1\,,\ \theta = 1\ \ at\ r = \eta, \tag{5.5}$$

$$\psi = \frac{F}{2},\ \psi = 1,\ \theta = 0\ \ at\ r = -\eta, \tag{5.6}$$

Introducing stream function $\psi(x, y, t)$ one can express

$$u = -\frac{\partial\psi}{\partial r},\qquad v = \frac{k\delta}{r+k}\frac{\partial\psi}{\partial x}.$$

After applying long wavelength and low Reynolds number assumptions equation (5.4) become

$$\frac{\partial}{\partial r}\left[\frac{1}{k(r+k)}\frac{\partial}{\partial r}\left\{(r+k)^2 S_{rx} + M^2\frac{\partial\psi}{\partial r}\right\}\right] = 0, \tag{5.7}$$

$$S_{rx} = \left(-\psi_{rr} + \frac{\psi_r}{r+k}\right)\left[1 - \xi\left(-\psi_{rr} + \frac{\psi_r}{r+k}\right)^2\right]^{-1}, \tag{5.8}$$

where $\xi = (\mu_1^2 - \lambda_1^2)$ is the pseudoplastic fluid parameter.

$$F = \int_{-\eta}^{\eta}\frac{\partial\psi}{\partial r}dr. \tag{5.9}$$

Using the small parameter ξ, we open the perturbation series defined as

$$\psi = \psi_0 + \xi\psi_1 + \cdots \tag{5.10}$$

$$S_{rx} = S_{0rx} + \xi S_{1rx} + \cdots \tag{5.11}$$

$$F = F_0 + \xi F_1 + \cdots \tag{5.12}$$

5.2.1: Zero order solution

Putting above expression in Equation (5.5), then comparing the coefficient of ξ^0 , we get

$$\frac{\partial}{\partial r}\frac{1}{k(r+k)}\frac{\partial}{\partial r}\left\{(r+k)^2 S_{0rx} + M^2\frac{\partial \psi_0}{\partial r}\right\} = 0, \tag{5.13}$$

$$S_{0rx} = \frac{\psi_{0r}}{r+k} - \psi_{0rr}\,.$$

The dimensionless boundary conditions are

$$\psi_0 = -\frac{F_0}{2},\ \ \psi_0 = 1,\ \theta_0 = 1,\ at\ r = \eta, \tag{5.14}$$

$$\psi_0 = \frac{F_0}{2},\ \ \psi_0 = 1,\ \theta_0 = 0\ \ at\ r = -\eta. \tag{5.15}$$

5.2.2: First order system

The first order system is given as:

$$\frac{\partial}{\partial r}\frac{1}{k(r+k)}\frac{\partial}{\partial r}\left\{(r+k)^2 S_{1rx} + M^2\frac{\partial \psi_1}{\partial r}\right\} = 0, \tag{5.16}$$

$$S_{1rx} = \frac{\psi_{1r}}{r+k} - \psi_{1rr} - \left(\frac{\psi_{0r}}{r+k} - \psi_{0rr}\right)^3,$$

with boundary conditions:

$$\psi_1 = -\frac{F_1}{2},\ \ \psi_1 = 0,\ \theta_1 = 0\ \ at\ r = \eta, \tag{5.17}$$

$$\psi_1 = \frac{F_1}{2},\ \ \psi_1 = 0,\ \theta_1 = 0\ \ at\ r = -\eta. \tag{5.18}$$

5.3 Entropy analysis

Entropy production or the pseudoplastic fluid can be defined as:

Entropy generation is:

$$S_{Gen} = \frac{\tilde{k}}{(\tilde{T}_{\widetilde{m}})^2}\left(\nabla\tilde{T}\right)^2 + \frac{1}{\tilde{T}_{\widetilde{m}}}\left(\tilde{S}.\tilde{L}\right), \tag{5.19}$$

$$S_{Gen} = \frac{\tilde{k}}{(\tilde{T}_{\widetilde{m}})^2}\left(\frac{\partial\tilde{T}}{\partial\tilde{r}} + \frac{\tilde{R}}{\tilde{r}+\tilde{R}}\frac{\partial\tilde{T}}{\partial\tilde{x}}\right)^2 + \frac{1}{\tilde{T}_{\widetilde{m}}}S_{XR}\left(\frac{\partial\tilde{u}}{\partial\tilde{R}} + \frac{\tilde{R}}{\tilde{r}+\tilde{R}}\frac{\partial\tilde{v}}{\partial X} - \frac{\tilde{u}}{\tilde{r}+\tilde{R}}\right) + \frac{\tilde{u}^2 {B_0}^2\tilde{\sigma}}{\tilde{T}_{\widetilde{m}}}\frac{\tilde{R}}{(\tilde{r}+\tilde{R})^2}, \tag{5.20}$$

In dimensionless form

$$N_s = \frac{S_{Gen}}{S_G} = \left(\frac{\partial\theta}{\partial r}\right)^2 + \frac{Br}{\wedge}S_{rx}\left(\frac{1}{r+k}\frac{\partial\psi}{\partial r} - \frac{\partial^2\psi}{\partial r^2}\right) + \left(\frac{kB}{K+r}\right)^2\left(\frac{\partial\psi}{\partial r}\right)^2, \tag{5.21}$$

with

$$S_G = \frac{k(T_1-T_0)}{(T_m)^2 d^2};\quad \wedge = \frac{(T_1-T_0)}{T_m}.$$

5.4 Results and Discussion

This segment provides an explanation of the results derived from Fig. 5.1 to 5.13. In this work magnetic fields were applied on a curved channel. The application of a magnetic field can exert forces on magnetic particles or ions in the fluid. This can influence the overall flow pattern within the curved channel. In the presence of a magnetic field, the Lorentz force may act on the conducting fluid, causing changes in velocity and pressure distribution. In a curved channel, peristaltic motion may be altered by the presence of a magnetic field. The magnetic forces may affect the propagation of peristaltic waves and the shape of the waves. The combination of peristaltic motion and magnetic forces can lead to complex fluid dynamics. The magnetic field may induce secondary flows, influencing the velocity and pressure distribution in the curved channel. The curvature of the channel can also affect the magnetic field distribution and, in turn, the magnetic forces acting on the fluid. Fig. 5.1 (a, b, and c) shows that when we apply a magnetic field on a curved channel the number of streamlines increases in the lower wall of the channel and decreases in the upper wall of the channel by increasing the value of magnetic field because when the effect of magnetic field increase then the bolus start to expand in the upper portion of the channel and this expansion decreases the number of streamline similarly in lower portion bolus contract and this contraction increases the number of streamline. Fig. 5.2 (a, b, and c) shows the variation of pseudoplastic parameter ξ on streamlines in a curved channel. An increasing value of $\xi > 0$ corresponds to an increase in the number of streamlines in the lower wall of the channel because the bolus starts to contract and decreases the number of streamlines in the upper wall of the channel by the expansion of the bolus. Fig. 5.3 (a, b, and c) shows the effect of curvature on streamlines. An increasing value of $k > 0$ corresponds to a decrease in the number of streamlines in the lower wall of the channel because the bolus starts to expand and an increase the number of streamlines in the upper wall of the channel by the contraction of the bolus. Fig. 5.4 shows the effect of the magnetic field on the velocity of a fluid in the curved channel. The primary effect of a magnetic field on a fluid is the generation of a Lorentz force. This force acts perpendicular to both the direction of the magnetic field and the direction of the current or fluid velocity (v). The Lorentz force acts as a constraint on fluid motion in the presence of a magnetic field, resulting in a drop in fluid velocity and an increase in flow resistance. The fluid velocity, fluid conductivity, and intensity of the magnetic field all affect how much magnetic braking occurs. As an increasing magnetic field intensity (B) is applied to a curved channel, fluid velocity decreases in the middle portion and increases in the higher and

lower areas. Fig 5.5 shows the effect of curvature on a velocity of a fluid. By increasing the value of curvature the velocity of a fluid decreases in lower portion and increases in upper portion of the channel. Fig 5.6 shows the effect of pseudoplastic parameter on a velocity of a fluid such that by increasing the value of pseudoplastic parameter velocity increase in upper portion and decreases in lower portion of the channel. Fig. 5.7 - 5.9 illustrates the impact of magnetic field strength (M), curvature (k), and fluid parameter (ξ) on fluid temperature. In Fig. 5.7, fluid temperature decreases in the central region of the channel and remains constant in the upper and lower regions. Fig. 5.8 demonstrates that an increase in curvature leads to a temperature decrease in the lower part and an increase in the upper part of the channel.

Fig. 5.9 shows that the temperature of a fluid increases by increases in Br number. Fig. 5.10 - 5.13 illustrates the impact of crucial parameters, namely M, ξ, Br, and k on the behavior of total entropy production (S). In Fig. 5.10 the influence of M on S is depicted, revealing an increase in entropy near the channel walls as M is heightened. The effect of Br on S is elucidated in Fig. 5.11, where the Brinkmann number Brelates to viscous effects and is directly proportional to the square of velocity. An increase in the Br number shows that the entropy increases in the upper and lower portions of the channel. Fig. 5.12 demonstrates the effect of ξ on S, indicating a decay in entropy in the vicinity of channel walls. Fig. 5.13 shows that the entropy increases in upper and lower with increasing the effect of k.

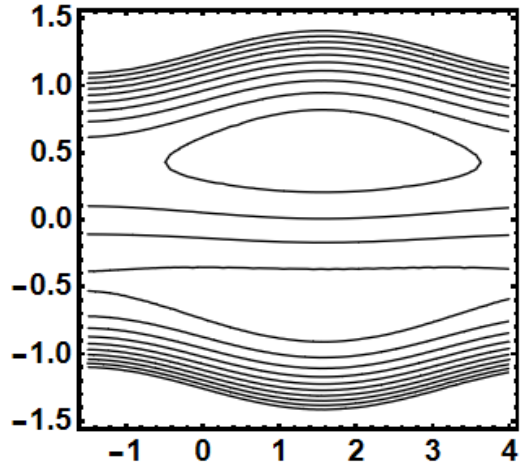

$(a) M = 0.1$

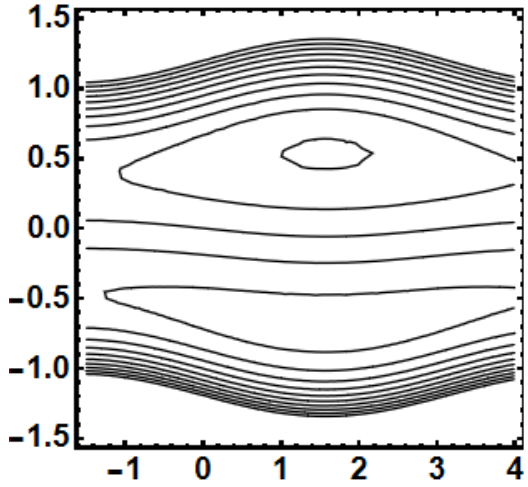

$(b) M = 5$

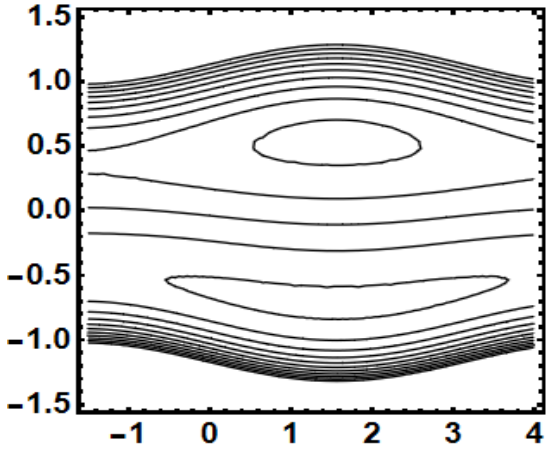

$(c) M = 7$

Fig 5.1: Variation of M on velocity of a fluid at M = 0.1, 5 and 7.

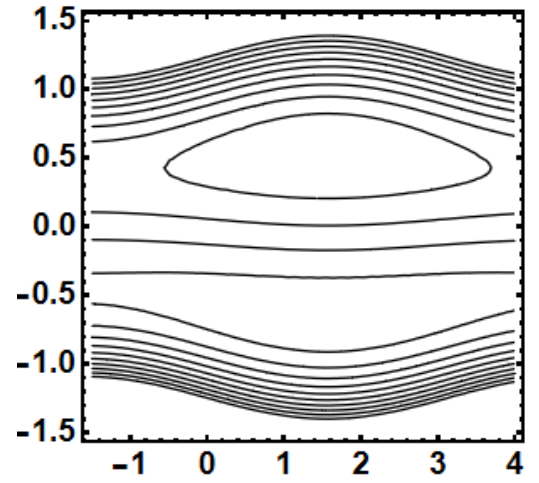

$(a)\xi = 0$

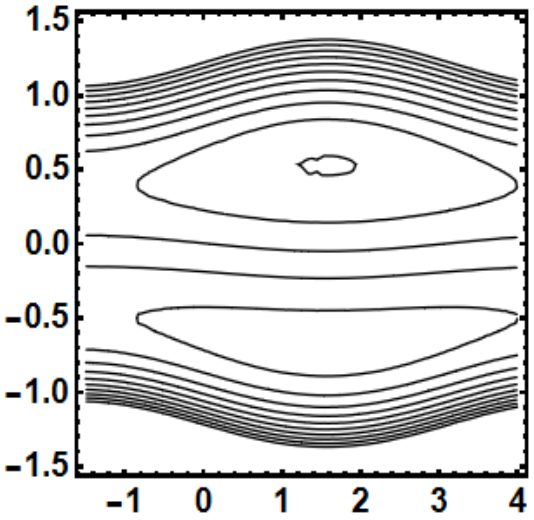

$(b)\xi = 0.02$

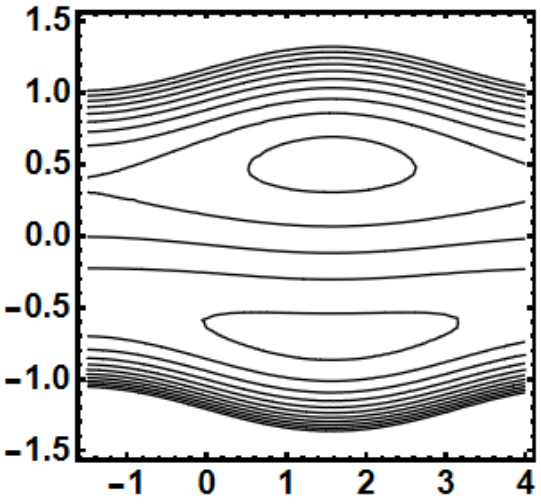

$(c)\xi = 0.04$

Fig 5.2: Variation ξ on velocity of a fluid at 0, 0.02 and 0.04.

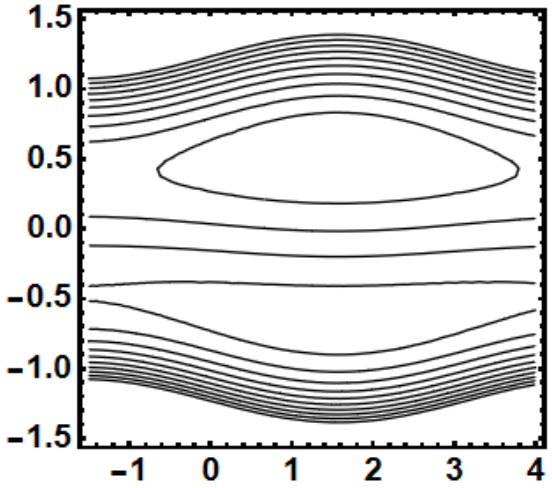

$(a) k = 3$

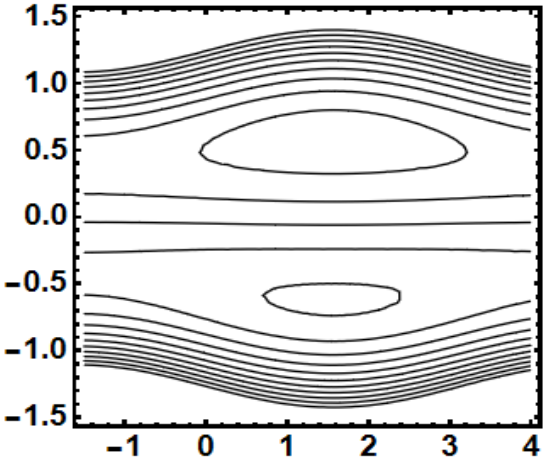

$(b) k = 8$

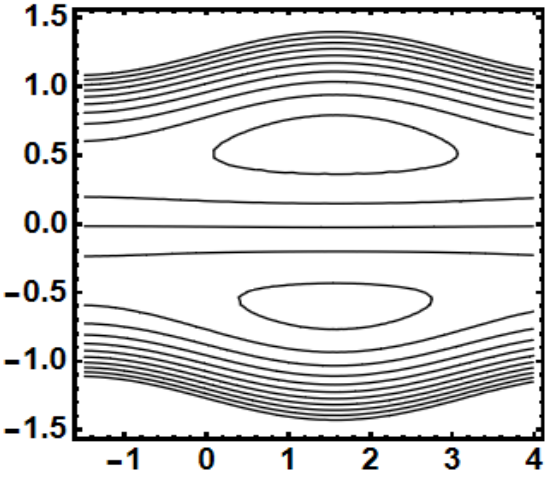

$(c) k = 16$

Fig 5.3: Variation of k on velocity of a fluid at 3, 8, and 16.

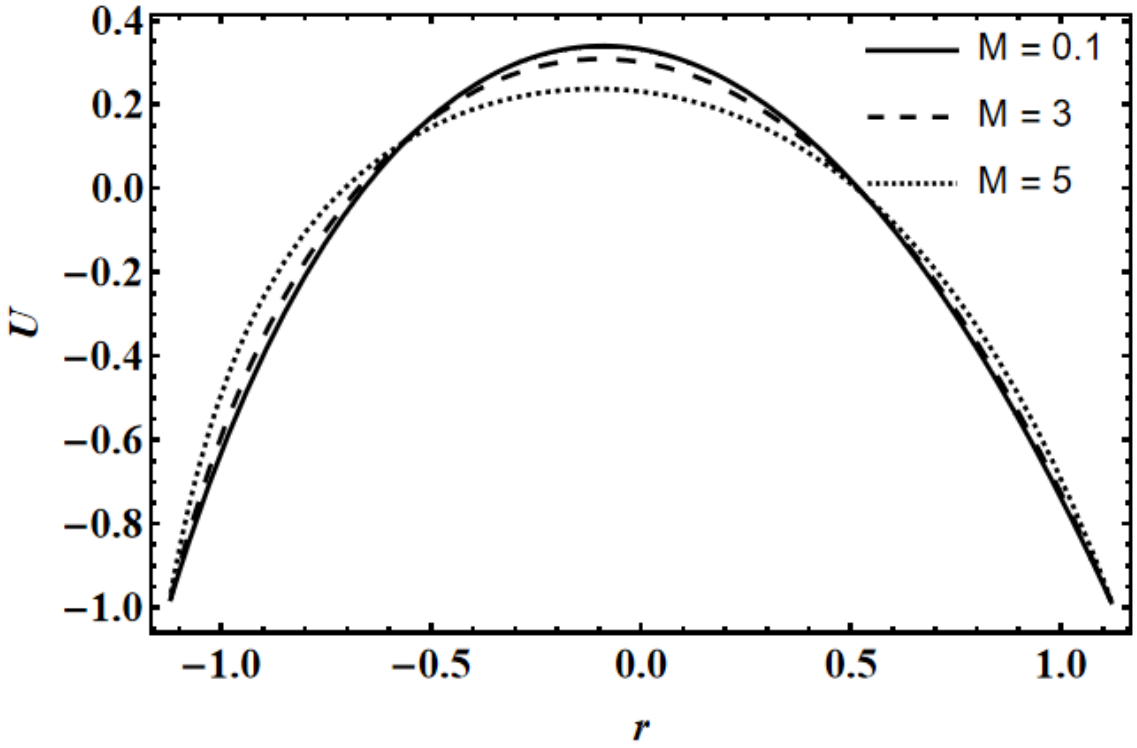

Fig 5.4: Variation of M on u at $M = 0.1, 3$ and 5.

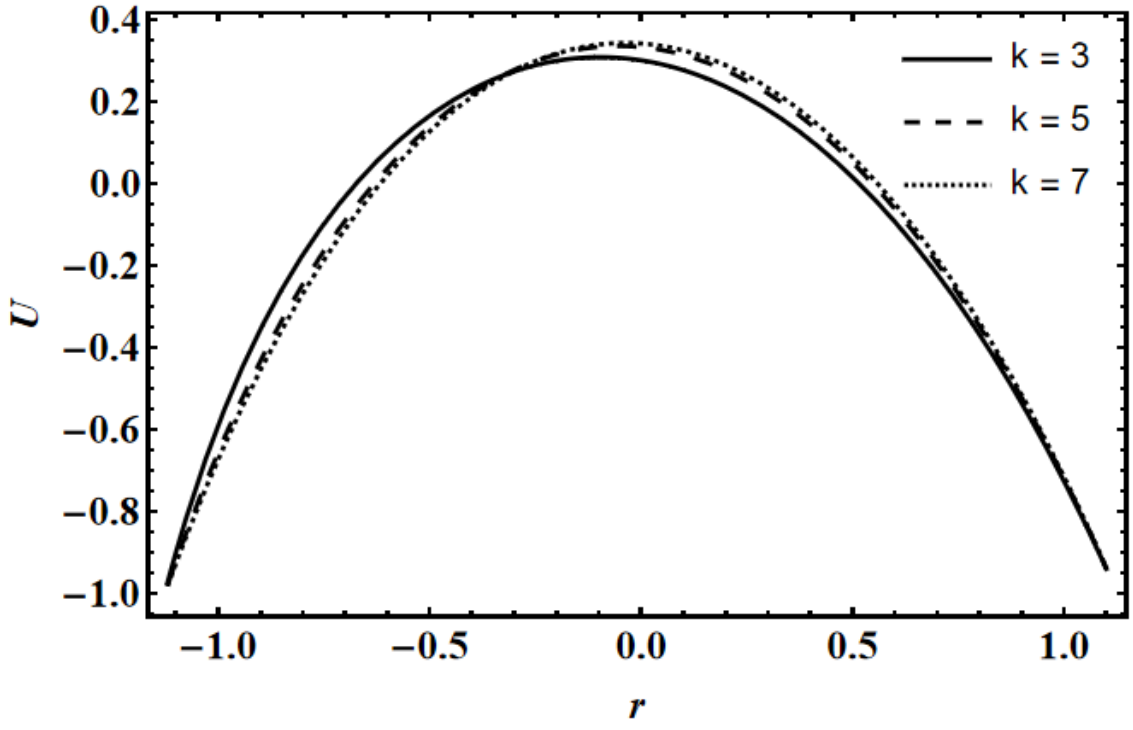

Fig 5.5: Variation of k on u at $k = 3, 5$ and 7.

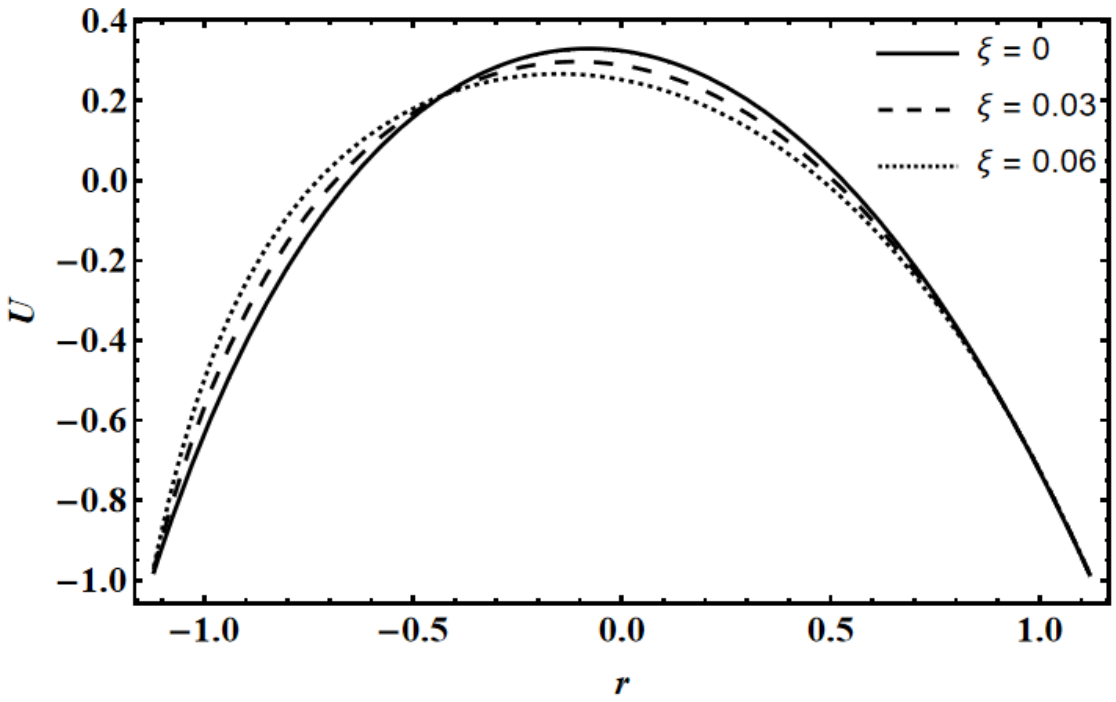

Fig 5.6: Variation of ξ on r at ξ = 0, 0.03, and 0.06.

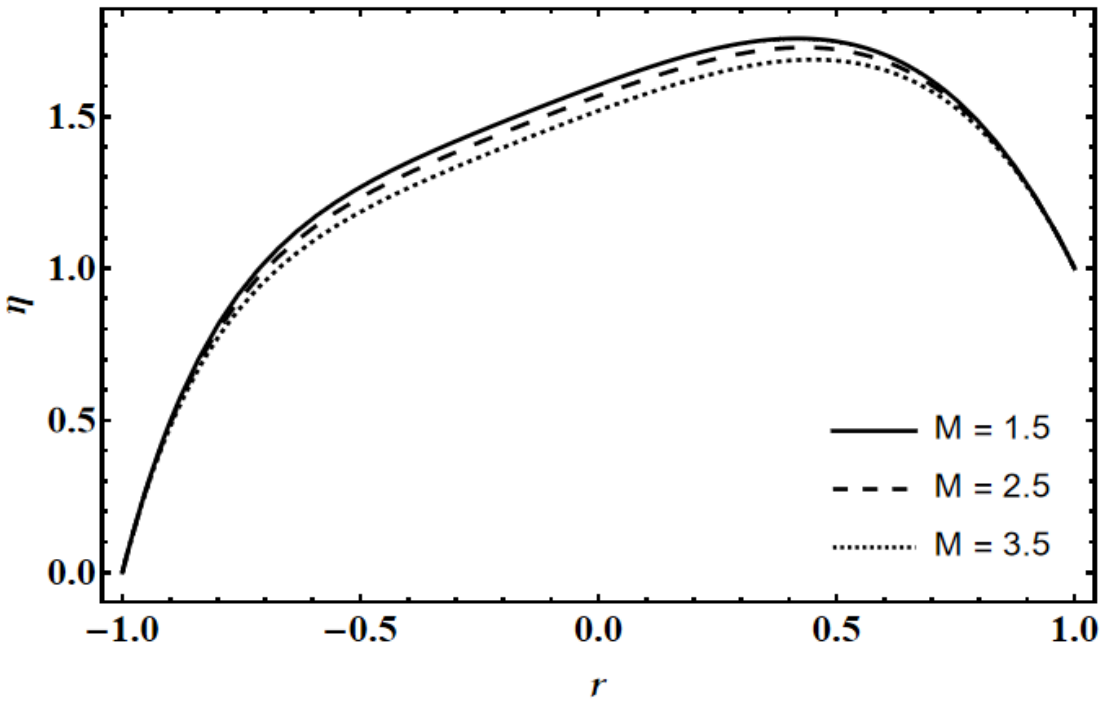

Fig 5.7: Variation of M on a temperature of a fluid at $M = 1.5, 2.5$, and 3.5.

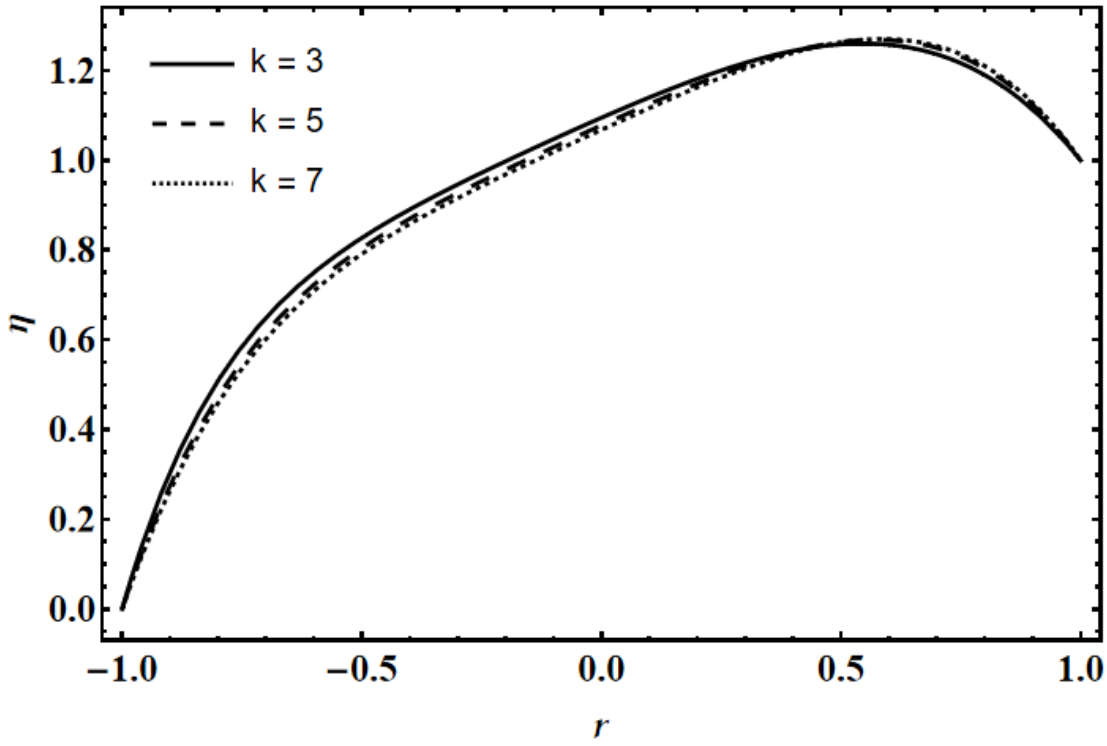

Fig 5.8: Variation of *k* on a temperature of a fluid at $k = 3, 5$ and 7

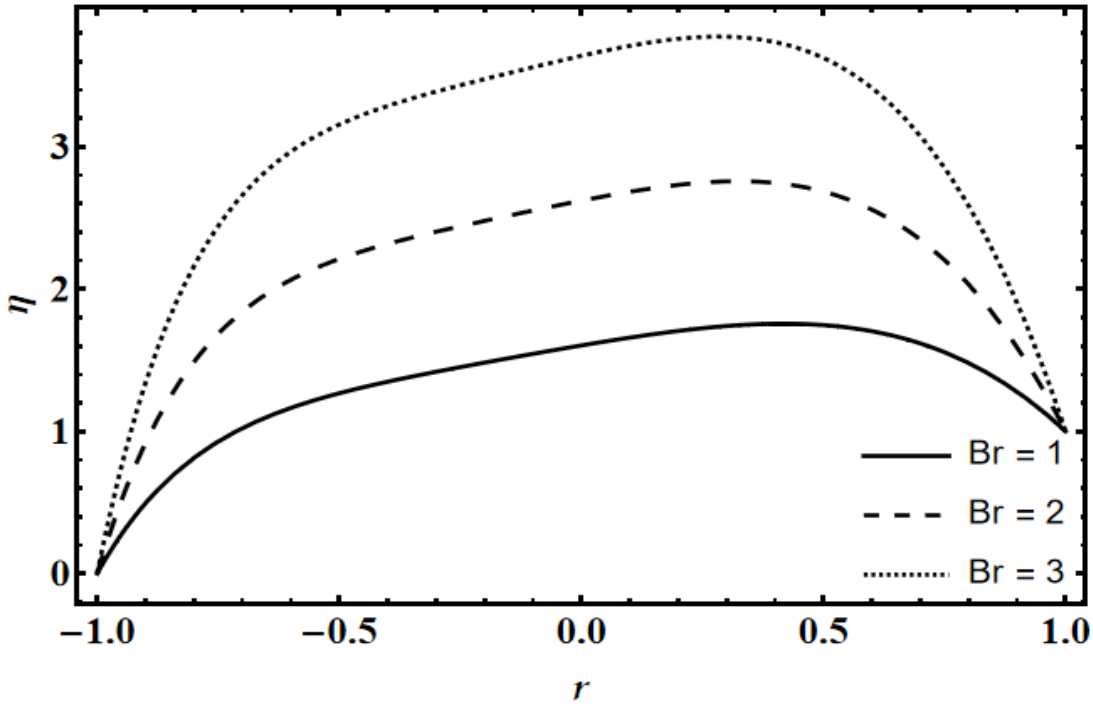

Fig 5.9: Variation of *Br* on a temperature of a fluid at $Br = 1,\ 2$ and 3

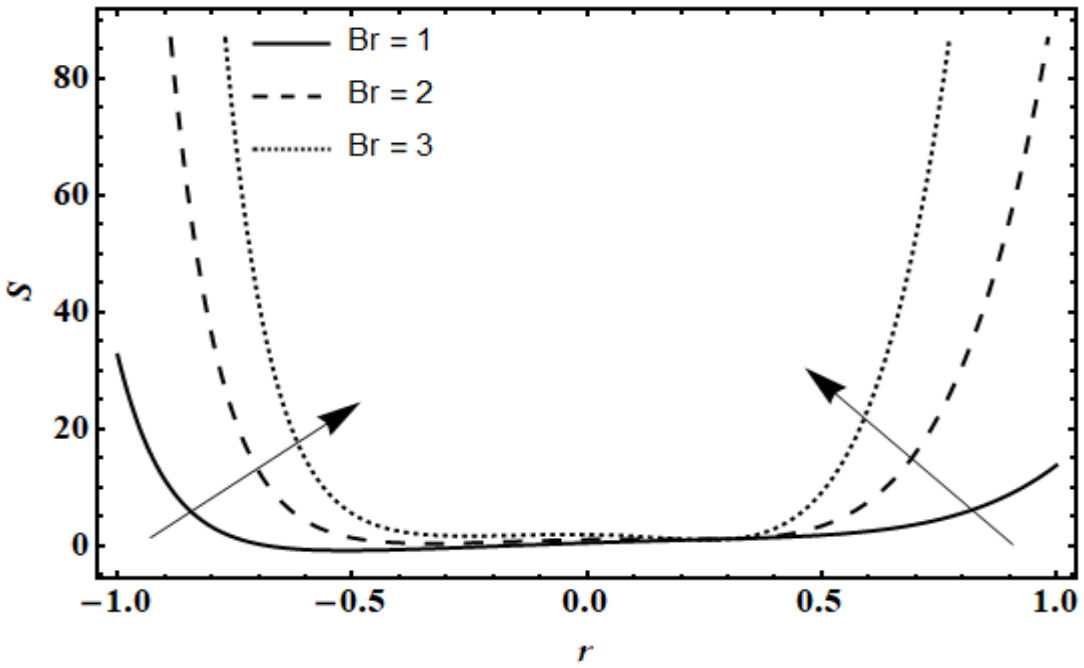

Fig 5.10: Variation of *Br* on *S* at $Br = 1, 2$ and 3.

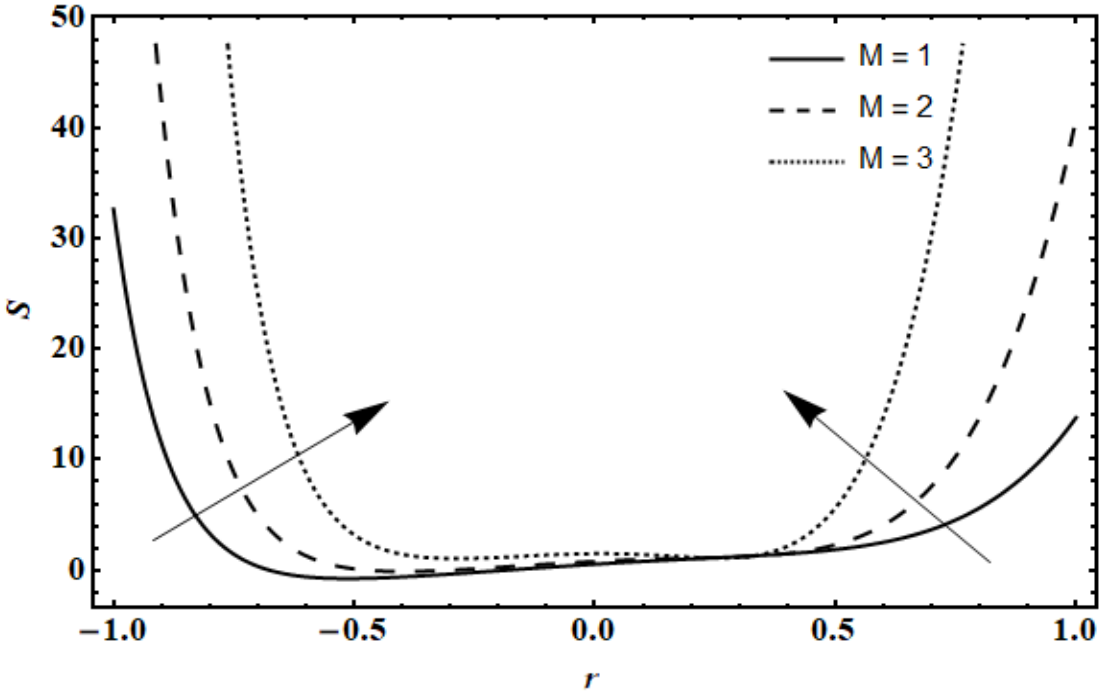

Fig 5.11: Variation of *M* on *S* at $M = 1, 2$ and 3.

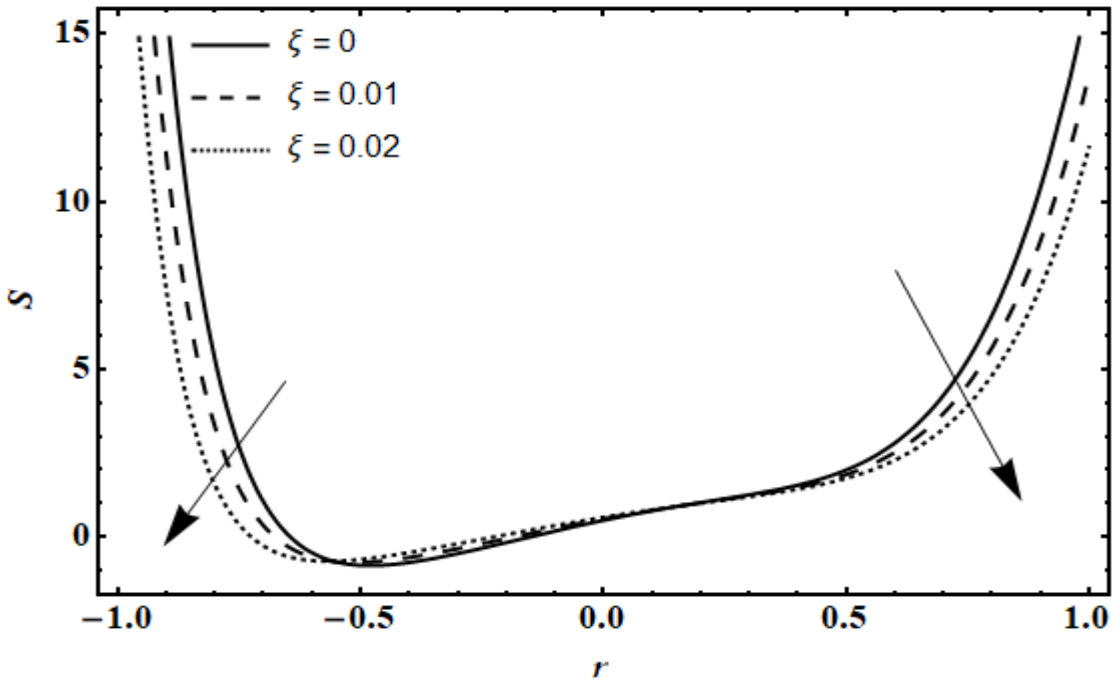

Fig 5.12: Variation of ξ on S at $\xi = 0, 0.01$ and 0.02

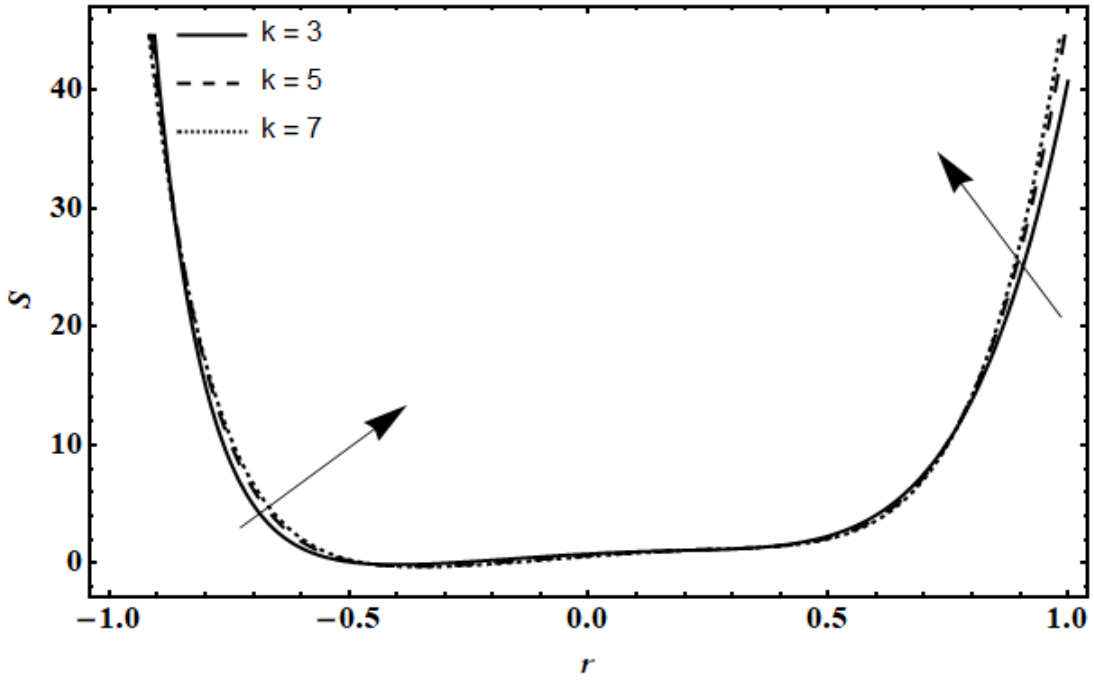

Fig 5.13: Variation of k on S at $k = 3, 5$ and 7

CHAPTER 6

CONCLUSION AND FUTURE WORK

6.1 Conclusion

The research investigates the impact of MHD effects on the peristaltic motion of a pseudoplastic fluid within a curved channel, accounting for entropy generation. By using perturbation method, the study derives analytical expressions for the stream function.

The following is a summary of the study's main findings: Asymmetry may be seen in the velocity profiles along the curved channel's line, which deviates from patterns seen in flat channels. Trapped boluses show increased size and circulation with increasing curvature parameter in the top portion of the channel, whereas the reverse tendency is observed in the bottom segment. This suggests that blood flow patterns in the top and lower portions of the artery are specifically influenced by the curvature parameter. Additionally, an increase in the curvature value results in a reduction in fluid velocity. in the upper portion and an increase in the lower portion. The introduction of magnetic effects follows a similar trend, where an increase in the magnetic field diminishes fluid velocity in the upper portion and enhances it in the lower portion. An elevation in M is shown to correspond with an increase in entropy along the channel walls, as seen by the link between variable M and entropy S. The influence of variable Br on entropy is explained; viscous effects are correlated with the Brinkmann number Br, which is directly proportional to the square of velocity. An increase in the Br number indicates an increase in entropy in the channel's upper and lower portions. An entropy reduction near the channel walls is suggested by the influence of variable ξ on entropy. To sum up, higher M causes entropy to grow along the channel walls, higher Br numbers raise entropy in the upper and lower channel sections, and the variable causes entropy to decrease near channel walls.

6.2 Future work

The complexity of the issue could be further explored by incorporating various fluid models, including Maxwell, Williamson, Burger, Jeffery, and tangent hyperbolic nanofluid. Additionally, factors such as nth order chemical reactions, activation energy, viscous dissipation, and the presence of solid particles can be taken into consideration for a comprehensive analysis. Further the effect of MHD will be applied on planner channel with inclined magnetic field. To address the aforementioned problem, alternative approaches may involve the exploration of diverse geometries such as wedges, cones, and cylinders.

REFERENCES

1. Saleem, A., Akhtar, S., Nadeem, S., Alharbi, F. M., Ghalambaz, M., & Issakhov, A. (2020). Mathematical computations for peristaltic flow of heated non-Newtonian fluid inside a sinusoidal elliptic duct. *Physica Scripta*, *95*(10), 105009.
2. Gudekote, M., Vaidya, H., Baliga, D., Choudhari, R., Prasad, K. V., & Viharika, V. (2019). The effects of convective and porous conditions on peristaltic transport of non-Newtonian fluid through a non-uniform channel with wall properties. *Journal of Advanced Research in Fluid Mechanics and Thermal Sciences*, *63*(1), 52-71.
3. Hina, S., Mustafa, M., Hayat, T., & Alsaedi, A. (2013). Peristaltic flow of pseudoplastic fluid in a curved channel with wall properties. *Journal of Applied Mechanics*, *80*(2), 024501.
4. Vaidya, H., Rajashekhar, C., Manjunatha, G., & Prasad, K. V. (2019). Peristaltic mechanism of a Rabinowitsch fluid in an inclined channel with complaint wall and variable liquid properties. *Journal of the Brazilian Society of Mechanical Sciences and Engineering*, *41*, 1-14.
5. Ali, N., Sajid, M., Abbas, Z., & Javed, T. (2010). Non-Newtonian fluid flow induced by peristaltic waves in a curved channel. *European Journal of Mechanics-B/Fluids*, *29*(5), 387-394.
6. Rashid, M., Ansar, K., & Nadeem, S. (2020). Effects of induced magnetic field for peristaltic flow of Williamson fluid in a curved channel. *Physica A: Statistical Mechanics and its Applications*, *553*, 123979.
7. Rashed, Z. Z., & Ahmed, S. E. (2021). Peristaltic flow of dusty nanofluids in curved channels. *Comput. Mater. Continua*, *66*(1), 1012-1026.
8. Noreen, S., Zahra, M., & Lu, D. C. (2022). Pseudoplastic fluid flow via electroosmotic and peristaltic pumping. *Waves in Random and Complex Media*.
9. Al-Zubaidi, A., Nazeer, M., Khalid, K., Yaseen, S., Saleem, S., & Hussain, F. (2021). Thermal analysis of blood flow of Newtonian, pseudo-plastic, and dilatant fluids through an inclined wavy channel due to metachronal wave of cilia. *Advances in Mechanical Engineering*, *13*(9), 16878140211049060.
10. Salman, M. R. (2023, February). Effect of convective conditions in a radiative peristaltic flow of pseudoplastic nanofluid through a porous medium in a tapered an inclined asymmetric channel. In *AIP Conference Proceedings* (Vol. 2414, No. 1). AIP Publishing.
11. Akhtar, S., Almutairi, S., & Nadeem, S. (2022). Impact of heat and mass transfer on the Peristaltic flow of non-Newtonian Casson fluid inside an elliptic conduit: Exact solutions through novel technique. *Chinese Journal of Physics*, *78*, 194-206.
12. Tanveer, A., Mahmood, S., Hayat, T., & Alsaedi, A. (2021). On electroosmosis in peristaltic activity of MHD non-Newtonian fluid. *Alexandria Engineering Journal*, *60*(3), 3369-3377.
13. Hasen, S. S., & Abdulhadi, A. M. (2020). MHD effect on peristaltic transport for rabinowitsch fluid through a porous medium in cilia channel. *Iraqi Journal of Science*, 1461-1472.

14. Rashid, M., Ansar, K., & Nadeem, S. (2020). Effects of induced magnetic field for peristaltic flow of Williamson fluid in a curved channel. *Physica A: Statistical Mechanics and its Applications*, *553*, 123979.
15. Chu, Y. M., Nazeer, M., Khan, M. I., Ali, W., Zafar, Z., Kadry, S., & Abdelmalek, Z. (2020). Entropy analysis in the Rabinowitsch fluid model through inclined Wavy Channel: Constant and variable properties. *International Communications in Heat and Mass Transfer*, *119*, 104980.
16. Naz, R., Noor, M., Shah, Z., Sohail, M., Kumam, P., & Thounthong, P. (2020). Entropy generation optimization in MHD pseudoplastic fluid comprising motile microorganisms with stratification effect. *Alexandria Engineering Journal*, *59*(1), 485-496.
17. Nadeem, S., Akhtar, S., Alharbi, F. M., Saleem, S., & Issakhov, A. (2022). Analysis of heat and mass transfer on the peristaltic flow in a duct with sinusoidal walls: Exact solutions of coupled PDEs. *Alexandria Engineering Journal*, *61*(5), 4107-4117.
18. Ali, N., Sajid, M., Javed, T., & Abbas, Z. (2010). Heat transfer analysis of peristaltic flow in a curved channel. *International Journal of Heat and Mass Transfer*, *53*(15-16), 3319-3325.
19. Singh, U. P., Medhavi, A., Gupta, R. S., & Bhatt, S. S. (2018). Theoretical study of heat transfer on peristaltic transport of Non-Newtonian fluid flowing in a channel: Rabinowitsch fluid model. *International Journal of Mathematical, Engineering and Management Sciences*, *3*(4), 450.
20. Magesh, A., & Kothandapani, M. (2021). Heat and mass transfer analysis on non-Newtonian fluid motion driven by peristaltic pumping in an asymmetric curved channel. *The European Physical Journal Special Topics*, *230*(5), 1447-1464.
21. Vaidya, H., Rajashekhar, C., Manjunatha, G., & Prasad, K. V. (2019). Effect of variable liquid properties on peristaltic flow of a Rabinowitsch fluid in an inclined convective porous channel. *The European Physical Journal Plus*, *134*, 1-14.
22. Rajashekhar, C., Manjunatha, G., Vaidya, H., Divya, B., & Prasad, K. (2018). Peristaltic flow of Casson liquid in an inclined porous tube with convective boundary conditions and variable liquid properties. *Frontiers in Heat and Mass Transfer (FHMT)*, *11*.
23. Devaki, P., Sreenadh, S., Vajravelu, K., Prasad, K. V., & Vaidya, H. (2018). Wall properties and slip consequences on peristaltic transport of a casson liquid in a flexible channel with heat transfer. *Applied Mathematics and Nonlinear Sciences*, *3*(1), 277-290.
24. Sadaf, H., Akbar, M. U., & Nadeem, S. (2018). Induced magnetic field analysis for the peristaltic transport of non-Newtonian nanofluid in an annulus. *Mathematics and Computers in Simulation*, *148*, 16-36.
25. Abbasi, F. M., Hayat, T., & Alsaedi, A. (2015). Numerical analysis for MHD peristaltic transport of Carreau–Yasuda fluid in a curved channel with Hall effects. *Journal of Magnetism and Magnetic Materials*, *382*, 104-110.
26. Hatami, M., Mosayebidorcheh, S., & Jing, D. (2019). Peristaltic flow and heat transfer of nanofluids in a sinusoidal wall channel: two-phase analytical study. *The Journal of Analysis*, *27*, 913-929.
27. Hafez, N. M., Alsemiry, R. D., Alharbi, S. A., & Abd-Alla, A. M. (2022). Peristaltic transport characteristics of a second-grade dusty fluid flown with heat transfer through a tube revisited. *Scientific Reports*, *12*(1), 21605.
28. Saba, Abbasi, F. M., & Shehzad, S. A. (2020). Impact of curvature-dependent channel walls on peristaltic flow of Newtonian fluid through a curved channel with heat transfer. *Arabian Journal for Science and Engineering*, *45*, 9037-9044.

29. Mallick, B., & Misra, J. C. (2019). Peristaltic flow of Eyring-Powell nanofluid under the action of an electromagnetic field. *Engineering Science and Technology, an International Journal*, *22*(1), 266-281.
30. Rafiq, M., Sajid, M., Alhazmi, S. E., Khan, M. I., & El-Zahar, E. R. (2022). MHD electroosmotic peristaltic flow of Jeffrey nanofluid with slip conditions and chemical reaction. *Alexandria Engineering Journal*, *61*(12), 9977-9992.
31. Naz, R., Tariq, S., Sohail, M., & Shah, Z. (2020). Investigation of entropy generation in stratified MHD Carreau nanofluid with gyrotactic microorganisms under Von Neumann similarity transformations. *The European Physical Journal Plus*, *135*(2), 178.
32. Tanveer, A., Hayat, T., Alsaedi, A., & Ahmad, B. (2019). Heat transfer analysis for peristalsis of MHD Carreau fluid in a curved channel through modified Darcy law. *Journal of Mechanics*, *35*(4), 527-535.
33. Tariq, H., & Khan, A. A. (2020). Peristaltic transport of a second-grade dusty fluid in a tube. *J. Mech. Eng. Res*, *11*(2), 11-25.
34. Manjunatha, G., Rajashekhar, C., Vaidya, H., Prasad, K. V., & Vajravelu, K. (2020). Impact of heat and mass transfer on the peristaltic mechanism of Jeffery fluid in a non-uniform porous channel with variable viscosity and thermal conductivity. *Journal of Thermal Analysis and Calorimetry*, *139*, 1213-1228.
35. Yasmin, H., Iqbal, N., & Hussain, A. (2020). Convective heat/mass transfer analysis on Johnson-Segalman fluid in a symmetric curved channel with peristalsis: engineering applications. *Symmetry*, *12*(9), 1475.
36. Gnaneswara Reddy, M., Venugopal Reddy, K., & Makinde, O. D. (2017). Heat transfer on MHD peristaltic rotating flow of a Jeffrey fluid in an asymmetric channel. *International Journal of Applied and Computational Mathematics*, *3*, 3201-3227.
37. Javed, M., & Hayat, T. (2017, January). Effects of heat transfer on MHD peristaltic transport of dusty fluid in a flexible channel. In *2017 14th international Bhurban conference on applied sciences and technology (IBCAST)* (pp. 539-550). IEEE.
38. Shukla, R., Medhavi, A., Bhatt, S. S., & Kumar, R. (2020). Mathematical analysis of heat transfer in peristaltic transport through a rough nonuniform inclined channel. *Mathematical Problems in Engineering*, *2020*.
39. Hayat, T., Farooq, S., & Alsaedi, A. (2017). MHD peristaltic flow in a curved channel with convective condition. *Journal of Mechanics*, *33*(4), 483-499.
40. Bhatt, S. S., Medhavi, A., Gupta, R. S., & Singh, U. P. (2017). Effects of heat transfer during peristaltic transport in nonuniform channel with permeable walls. *Continuity*, *2*(Y2), 3.
41. Eldabe, N. T., Moatimid, G. M., Abouzeid, M. Y., ElShekhipy, A. A., & Abdallah, N. F. (2020). A semianalytical technique for MHD peristalsis of pseudoplastic nanofluid with temperature-dependent viscosity: Application in drug delivery system. *Heat Transfer—Asian Research*, *49*(1), 424-440.
42. Tahir, M., Ahmad, A., & Shehzad, S. A. (2022). Study of pseudoplastic and dilatant behavior of nanofluid in peristaltic flow: Reiner-Philippoff models. *Chinese Journal of Physics*, *77*, 2371-2388.
43. Devakar, M., Ramesh, K., & Vajravelu, K. (2022). Magnetohydrodynamic effects on the peristaltic flow of couple stress fluid in an inclined tube with endoscope. *Journal of Computational Mathematics and Data Science*, *2*, 100025.
44. Abbas, Z., Rafiq, M. Y., Alshomrani, A. S., & Ullah, M. Z. (2021). Analysis of entropy generation on peristaltic phenomena of MHD slip flow of viscous fluid in a diverging tube. *Case Studies in Thermal Engineering*, *23*, 100817.

45. Shehzad, S. A., Madhu, M., Shashikumar, N. S., Gireesha, B. J., & Mahanthesh, B. (2021). Thermal and entropy generation of non-Newtonian magneto-Carreau fluid flow in microchannel. *Journal of Thermal Analysis and Calorimetry*, *143*, 2717-2727.
46. Rooman, M., Jan, M. A., Shah, Z., Kumam, P., & Alshehri, A. (2021). Entropy optimization and heat transfer analysis in MHD Williamson nanofluid flow over a vertical Riga plate with nonlinear thermal radiation. *Scientific Reports*, *11*(1), 18386.
47. Hou, E., Hussain, A., Rehman, A., Baleanu, D., Nadeem, S., Matoog, R. T., ... & Sherif, E. S. M. (2021). Entropy generation and induced magnetic field in pseudoplastic nanofluid flow near a stagnant point. *Scientific Reports*, *11*(1), 23736.
48. Rashid, M., Ansar, K., & Nadeem, S. (2020). Effects of induced magnetic field for peristaltic flow of Williamson fluid in a curved channel. *Physica A: Statistical Mechanics and its Applications*, *553*, 123979.
49. Hasen, S. S., & Abdulhadi, A. M. (2020, October). Heat and mass impacts on peripheral layers of different viscosity on peristaltic flow of Rabinowitsch fluids. In *AIP Conference Proceedings* (Vol. 2292, No. 1, p. 020007). AIP Publishing LLC.
50. Hasona, W. M., Almalki, N. H., ElShekhipy, A. A., & Ibrahim, M. G. (2020). Combined effects of variable thermal conductivity and electrical conductivity on peristaltic flow of pseudoplastic nanofluid in an inclined non-Uniform asymmetric channel: Applications to solar collectors. *Journal of Thermal Science and Engineering Applications*, *12*(2).
51. Abd-Alla, A. M., Abo-Dahab, S. M., Thabet, E. N., & Abdelhafez, M. A. (2022). Heat and mass transfer for MHD peristaltic flow in a micropolar nanofluid: mathematical model with thermophysical features. *Scientific Reports*, *12*(1), 21540.
52. Hayat, T., Iqbal, R., Tanveer, A., & Alsaedi, A. (2016). Soret and Dufour effects in MHD peristalsis of pseudoplastic nanofluid with chemical reaction. *Journal of Molecular Liquids*, *220*, 693-706.
53. El-Dabe, N. T., Abou-Zeid, M. Y., Mohamed, M. A., & Abd-Elmoneim, M. M. (2021). MHD peristaltic flow of non-Newtonian power-law nanofluid through a non-Darcy porous medium inside a non-uniform inclined channel. *Archive of Applied Mechanics*, *91*, 1067-1077.
54. Hayat, T., Nisar, Z., Alsaedi, A., & Ahmad, B. (2021). Analysis of activation energy and entropy generation in mixed convective peristaltic transport of Sutterby nanofluid. *Journal of Thermal Analysis and Calorimetry*, *143*, 1867-1880.
55. Akbarzadeh, M., Rashidi, S., & Esfahani, J. A. (2017). Influences of corrugation profiles on entropy generation, heat transfer, pressure drop, and performance in a wavy channel. *Applied Thermal Engineering*, *116*, 278-291.
56. Khan, M. I., Alzahrani, F., Hobiny, A., & Ali, Z. (2020). Estimation of entropy generation in Carreau-Yasuda fluid flow using chemical reaction with activation energy. *Journal of Materials Research and Technology*, *9*(5), 9951-9964.
57. Iqbal, J., & Abbasi, F. M. (2022). Analysis of entropy generation for Magnetohydrodynamics peristaltic motion of Carreau-Yasuda nanofluid through a curved channel with variable thermal conductivity and Joule heating. *Waves in Random and Complex Media*, 1-20.
58. Hayat, T., Khan, A. A., Bibi, F., & Alsaedi, A. (2021). Entropy minimization for magneto peristaltic transport of Sutterby materials subject to temperature dependent thermal conductivity and non-linear thermal radiation. *International Communications in Heat and Mass Transfer*, *122*, 105009.

59. Ahmed, B., Hayat, T., Abbasi, F. M., & Alsaedi, A. (2021). Mixed convection and thermal radiation effect on MHD peristaltic motion of Powell-Eyring nanofluid. *International Communications in Heat and Mass Transfer*, *126*, 105320.
60. Bibi, F., Hayat, T., Farooq, S., Khan, A. A., & Alsaedi, A. (2021). Entropy generation analysis in peristaltic motion of Sisko material with variable viscosity and thermal conductivity. *Journal of Thermal Analysis and Calorimetry*, *143*, 363-375.
61. Alsaedi, A., Nisar, Z., Hayat, T., & Ahmad, B. (2021). Analysis of mixed convection and hall current for MHD peristaltic transport of nanofluid with compliant wall. *International Communications in Heat and Mass Transfer*, *121*, 105121.
62. Javid, K., Ali, N., & Asghar, Z. (2019). Numerical simulation of the peristaltic motion of a viscous fluid through a complex wavy non-uniform channel with magnetohydrodynamic effects. *Physica Scripta*, *94*(11), 115226.
63. Tariq, H., Khan, A. A., & Shah, S. (2023). Study of peristaltic transport of a dusty second-grade fluid in a curved configuration. *Scientia Iranica*.
64. Ellahi, R., Raza, M., & Akbar, N. S. (2017). Study of peristaltic flow of nanofluid with entropy generation in a porous medium. *Journal of Porous Media*, *20*(5).
65. Saba, S., Abbasi, F. M., & Shehzad, S. A. (2022). Influence of curvature-dependent channel walls on MHD peristaltic flow of viscous fluid with Hall currents and Joule dissipation. *Scientia Iranica*, *29*(6), 3107-3118.
66. Akbar, Y., & Abbasi, F. M. (2020). Impact of variable viscosity on peristaltic motion with entropy generation. *International Communications in Heat and Mass Transfer*, *118*, 104826.
67. Fluid Mechanics Hardcover – International Edition, August 1, 1980.
68. Hina, S., Mustafa, M., Hayat, T., & Alotaibi, N. D. (2015). On peristaltic motion of pseudoplastic fluid in a curved channel with heat/mass transfer and wall properties. *Applied Mathematics and Computation*, *263*, 378-391.